GGA GAC ATC TCG GAG GTA-3′ and 5′-GGC TCA CCA GTT TCA TTA GCA-3′), human LXRβ (5′-GCG AAG TTA CTT TTG AGG GTA-3′ and 5′-CTC CTT TAC AGT GGG TGA AGA-3′), human PPARα (5′-TCG GTG ACT TAT CCT GTG GTC-3′and 5′-TTC TCA GAT CTT GGC ATT CGT-3′), human PPARδ (5′-TCT CTC TTC CCT TCT CCC TTG-3′ and 5′-GGC TCA AGT CTT TTG CTC TGA-3′), human PPARγ (5′-TCA CAG AGT ATG CCA AAA GCA-3′and 5′-AAA CTC AAA CTT GGG CTC CAT-3′), mouse ABCA1 (5′-CTC AGA GGT GGC TCT GAT GAC-3′ and 5′-CCC ATA CAG CAA GAG CAG AAG-3′), mouse LXRα (5′-TAG GGA TAG GGT TGG AGT CAG-3′ and 5′-AGT TTC TTC AAG CGG ATC TGT-3′), mouse PPARα (5′-CTG TCC TCT CTC CCC ACT GGA-3′ and 5′-TGA CTG AGG AAG GGC TGG AAG-3′), mouse PPARδ (5′-GGG AAG AGG AGA AAG AGG AA-3′ and 5′-AGG AAG GGG AGG AAT TCT G-3′), mouse PPARγ (5′-ATA AAG CAT CAG GCT TCC ACT-3′and 5′-GCA CTT CTG AAA CCG ACA GTA-3′), human and mouse β-actin (5′-CTG ACC CTG AAG TAC CCC ATT-3′ and 5′-TCT GCG CAA GTT AGG TTT TGT-3′ (synthesized by Hokkaido System Science, Japan). Quantification of mRNA for these primers products were accomplished by using SYBR green PCR master mix reagent in an ABI PRISM 7700 sequence detection system (Applied Biosystem Japan). Results were normalized to β-actin mRNA.

2.5. RNA interference

Human LXRα-specific small interfering RNA (siRNA) and scrambled control RNA oligonucleotides were purchased from Invitrogen. The transfection of siRNA was performed using Nucleofector kit (Amaxa) reagent according to the manufacturer's instructions. Scrambled control RNA oligonucleotide or human LXRα siRNA were added to WI38 cells and transfected by electroporation. The cells were incubated for 20 h, and washed with PBS, then incubated in MEM containing 0.02% BSA and indicated dose of fenofibrate, bezafibrate, gemfibrozil, LY518674, GW501516, pioglitazone were added and incubated for further 20 h. Then the cells were harvested and mRNA levels determined by RT-PCR. The oligonucleotide sequences used to construct siRNA for LXRα in this study were: siLXRα (5′-UUC UCG AUC AUG CCC AGU UGU UCC G-3′) and scrambled control (5′-UUC UUC UUA GUA CCC GGA CGU UCC G-3′).

2.6. Construction of luciferase reporter genes

The construct of human PPARα promoter luciferase reporter gene (containing −1664/+83 of the PPARα gene, relative to the transcription start site) was prepared as described previously [25]. The 5′-flanking region of this PPARα gene (corresponding to −1664/+83) was inserted into pGL4 vector (Promega) to generate PPARα promotor-luciferase reporter construct (pPPARα-Luc). The reporter plasmid with a mutated and inactivated PPARα responsive element (PPRE) (mutant PPRE) was generated by using QuickChange Site-Directed Mutagenesis Kit (Stratagene). A mutation was introduced at the PPRE (−1493/−1481 GGGGCAAGTTCA to GcaGCAAGTTCA) which is identical to that reported previously (pPPARα-mut-Luc) [25]. The luciferase reporter plasmid was prepared to contain four copies of LXRE upstream of thymidine kinase promoter (pLXRE-tk-Luc) [26]. The sequence of LXRE of the LXRE-tk-Luc vector was (ACAG **TGACCG** CCAG **TAACCC** CAG...GGA **CGCCCG** CTAG **TAACCC** CGG) × 2 (LXREa and LXREb from sterol responsive element binding protein-1c).

2.7. Transient transfections and reporter gene assay

WI38 cells and mouse fibroblasts were co-transfected with pPPARα-Luc or pPPARα-mut-Luc vectors (4 μg), and Renilla phRL-tk vector (Promega) (0.2 μg) by electroporation using Nucleofector kit reagent (Amaxa) according to instructions supplied by the manufacturer. The activity of luciferase reporter of LXRE, pLXRE-tk-Luc, was examined in human fibroblasts and mouse fibroblasts of wild type and of PPARα(−/−). After 20 h transfection, the cells were washed with PBS and cultured in the presence of fenofibrate, bezafibrate, gemfibrogil, LY518674, GW 501516, pioglitazone for 20 h. Cellular luciferase activity was measured by the Dual-Luciferase Reporter Assay System (Promega). Results were standardized by the Renilla luciferase activity derived from phRL-tk vector.

2.8. Other methods

Protein content of each sample was determined with bicinchoninic acid assay reagent (Pierce) using BSA as a standard. Statistical significance was evaluated using two-tailed Student's *t* test and analysis of variance Scheffe's test.

3. Results

3.1. HDL biogenesis in THP-1 macrophages and WI38 fibroblasts

The effects of PPAR agonists on HDL biogenesis were determined by measuring the expression of ABCA1 and cellular lipid release by human apoA-I (Figs. 1 and 2). Fenofibrate, bezafibrate, gemfibrozil, LY518674, GW501516 and pioglitazone increased ABCA1 mRNA and protein levels and consequently cellular lipid release. In addition,

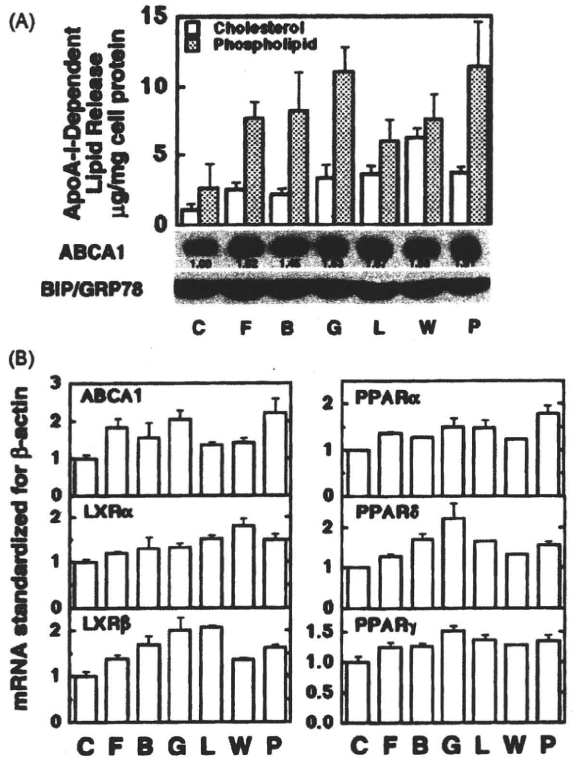

Fig. 1. Effects of PPARα agonists fenofibrate (F), bezafibrate (B), gemfibrozil (G) and LY518674 (L) at 30 μM, PPARδ agonist GW501516 (W) at 0.5 μM, and PPARγ agonist pioglitazone (P) at 5 μM, in comparison to control (C) in THP1 macrophages. The cells were exposed to PPAR agonists for 20 h. (A) ApoA-I-mediated release of free cholesterol and choline-phospholipid were measured in the conditioned medium as described in the text. ABCA1 protein was determined by immunoblotting after incubation with PPAR agonists for 20 h. The numbers in the ABCA1 immunoblotting photo indicate the results of digital densitometric scans of each band standardized for the loading standard and expressed as the relative value to the control. (B) Messenger RNA levels of ABCA1, LXRα, LXRβ, PPARα, PPARδ, PPARγ were determined by quantitative RT-PCR after incubation with PPAR agonists for 20 h and standardized with those of β-actin mRNA levels. Data represent mean ± S.E. of three independent measurements. All the data are statistically significant for the increase from the control as $P < 0.01$.

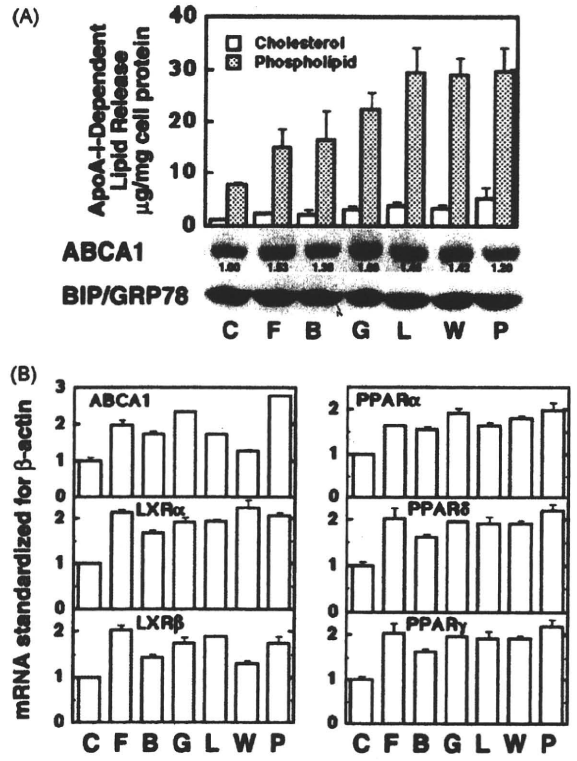

Fig. 2. Effects of PPARα agonists fenofibrate (F), bezafibrate (B), gemfibrozil (G) and LY518674 (L) at 30 μM, PPARδ agonist GW501516 (W) at 0.5 μM, and PPARγ agonist pioglitazone (P) at 5 μM, in comparison to control (C) in WI38 cells. The cells were exposed to PPAR agonists for 20 h. The numbers in the ABCA1 immunoblotting photo indicate the results of digital densitometric scan of each band standardized for the loading standard and expressed as the relative value to the control. (A) ApoA-I-mediated release of free cholesterol and choline-phospholipid were measured in the conditioned medium as described in the text. ABCA1 protein was determined by immunoblotting after incubation with PPAR agonists for 20 h. (B) Messenger RNA levels of ABCA1, LXRα, LXRβ, PPARα, PPARδ, PPARγ were measured by quantitative RT-PCR after incubation with PPAR agonists for 20 h and standardized for β-actin mRNA. Data represent mean ± S.E. of three independent measurements. All the data are statistically significant for the increase from the control as $P < 0.01$.

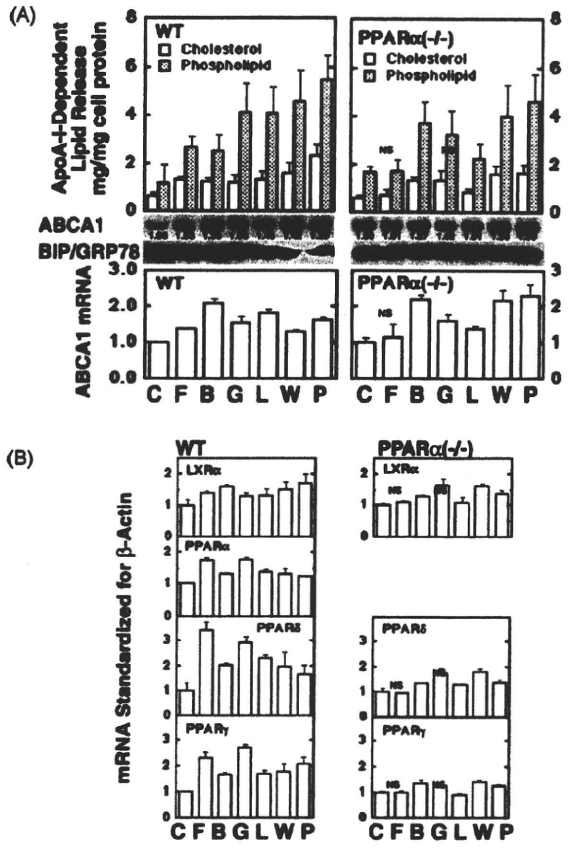

Fig. 3. Effects of PPARα agonists fenofibrate (F), bezafibrate (B), gemfibrozil (G) and LY518674 (L) at 30 μM, PPARδ agonist GW501516 (W) at 0.5 μM, and PPARγ agonist pioglitazone (P) at 5 μM, in comparison to control (C) in mouse fibroblasts, wild type (WT) and PPARα(−/−). The cells were exposed to PPAR agonists for 20 h. (A) ApoA-I-mediated release of free cholesterol and choline-phospholipid were measured in the conditioned medium as described in the text. ABCA1 protein and its mRNA standardized for those of β-actin were determined after incubation with PPAR agonists for 20 h. The numbers in the ABCA1 immunoblotting photo indicate the results of digital densitometric scan of each band standardized for the loading standard and expressed as the relative value to the control. (B) Messenger RNA levels of LXRα, LXRβ, PPARα, PPARδ, PPARγ were detected after incubation with PPAR agonists for 20 h and standardized for those of β-actin. Data represent mean ± S.E. of three independent measurements. All the data in the wild type fibroblasts are statistically significant for the increase from the control as $P < 0.01$. For those in PPARα(−/−) fibroblasts, no significant increase from the control is indicated as NS.

all compounds increased mRNAs coding LXRα, LXRβ, PPARα, PPARδ and PPARγ. The results were same with WI38 fibroblasts (Fig. 2). Therefore, activation of PPARs by their agonists results in transcriptional enhancement, not only of LXRα and ABCA1 but also LXRβ and PPARs themselves in these cell lines.

3.2. HDL biogenesis in PPARα null mouse fibroblasts

In order to differentiate a role of PPARα and other PPARs, a similar analysis was done using fibroblasts prepared from wild-type and PPARα(−/−) mice (Fig. 3). The increase in cellular lipid release was reduced in PPARα(−/−) cells by fenofibrate and LY518674. In contrast, PPARα deficiency only marginally influenced lipid release induced by bezafibrate, GW501516 and pioglitazone as expected since these compounds preferably activate PPARδ or PPARγ. These results also indicate that their effects are entirely or partially dependent on the presence of PPARα. Expression of ABCA1, as estimated by mRNA and protein expression was roughly parallel to the results of the lipid release. Increase of LXRα mRNA was also reduced in PPARα(−/−) cells in parallel with the ABCA1-related reactions. Increase of PPARδ and PPARγ mRNA was diminished when PPARα was knocked-out for all the ligands, suggesting that cis or trans activation of PPARs may require the presence of PPARα for its full activity.

3.3. PPARα promoter assay

In order to investigate the mechanism of PPARα induction, the PPARα promoter was investigated by transfected studies in WI38 cells. As shown in Fig. 4A, PPARα promoter activity was increased by all of the PPARs ligands, indicating trans activation of the PPARα gene by all PPAR subtypes. When the PPRE was mutated in the promoter, all of these effects were abolished. The PPARα promoter was also activated by TO901317, an LXR ligand indicating that activation depends on LXR. To confirm this finding, LXRα was down-regulated by a specific siRNA (by 80 ± 2% at 100 nM, based on standardization for β-actin). The activation by the PPAR ligands was eliminated under these conditions while transfection of scrambled siRNA had no effect (data not shown in Fig. 4A). The results therefore demonstrated that activation of PPARα by PPARs ligands requires both the PPRE-mediated activation by LXRα. PPARα promoter activity was also observed in mouse fibroblasts prepared from wild-type and in PPARα(−/−) mice. As shown in Fig. 4B, the activity was increased by all the ligands and the effects were reduced by introducing muta-

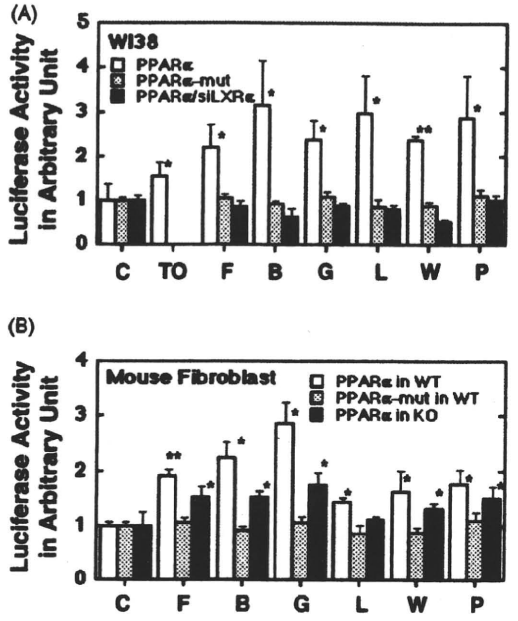

Fig. 4. Human PPARα promoter activity influenced by PPAR agonists. (A) Reporter gene construct of pPPARα-Luc and its mutant in PPRE (pPPARα-mut-Luc) were transfected for 20 h to WI38 cells or WI38 cells in which expression the LXRα gene was down-regulated by 80% by a specific siRNA (siLXRα), and the cells were incubated for further 20 h with an LXR agonist TO901317 (TO), PPARα agonists fenofibrate (F), bezafibrate (B), gemfibrozil (G) and LY518674 (L) at 30 μM, PPARδ agonist GW501516 (W) at 0.5 μM, and PPARγ agonist pioglitazone (P) at 5 μM, in comparison to control (C). The cells were lysed and firefly luciferase activity measured by the Dual-Luciferase Reporter Assay System (Promega). (B) Reporter gene construct of pPPARα-Luc and pPPARα-mut-Luc were transfected for 20 h to mouse fibroblasts of wild type (WT) and PPARα(−/−). After transfection the cells were incubated for further 20 h with PPARα agonists fenofibrate (F), bezafibrate (B), gemfibrozil (G) and LY518674 (L) at 30 μM, PPARδ agonist GW501516 (W) at 0.5 μM, and PPARγ agonist pioglitazone (P) at 5 μM, in comparison to control (C), and luciferase activity was determined. Results were standardized for Renilla luciferase activity derived from the phRL-tk vector. The values represent the average ± S.D. of three independent experiments performed in septuplicate. Significance of the increase from the control is indicated as $^{*}P < 0.05$ and $^{**}P < 0.01$.

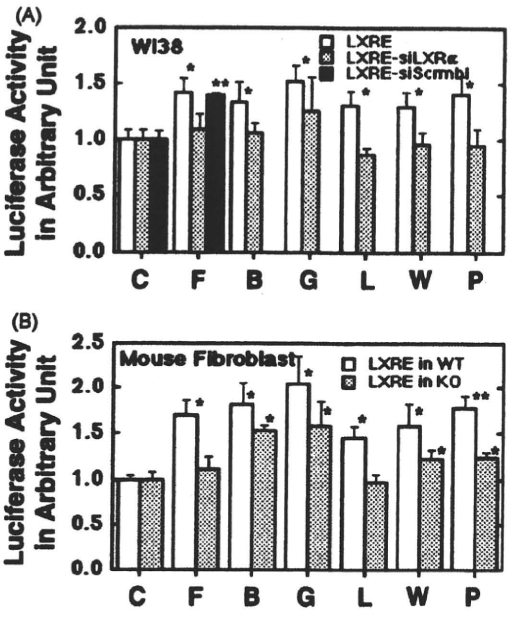

Fig. 5. Activity of the LXRα response element (LXRE)-containing reporter gene (pLXRE-tk-Luc) transcription influenced by PPAR agonists. (A) The luciferase reporter plasmid for LXRE (pLXRE-tk-Luc) was transfected with and without siRNA specific to LXRα (siLXRα) or its scramble control (siScrmbl) to WI38 cells for 20 h. The cells were incubated for further 20 h with PPARα agonists fenofibrate (F), bezafibrate (B), gemfibrozil (G) and LY518674 (L) at 30 μM, PPARδ agonist GW501516 (W) at 0.5 μM, and PPARγ agonist pioglitazone (P) at 5 μM, in comparison to control (C), luciferase activity was determined. B: The reporter gene pLXRE-tk-Luc was transfected to mouse fibroblasts, wild type (WT) and PPARα(−/−), for 20 h. The cells were incubated for 20 h with PPARα agonists fenofibrate (F), bezafibrate (B), gemfibrozil (G) and LY518674 (L) at 30 μM, PPARδ agonist GW501516 (W) at 0.5 μM, and PPARγ agonist pioglitazone (P) at 5 μM, in comparison to control (C), luciferase activity was determined. Results were standardized by the Renilla luciferase activity derived from phRL-tk vector. The values represent the average ± S.D. of three independent experiments performed in septuplicate. Significance of the increase from the controls is indicated as $^{*}P < 0.05$ and $^{**}P < 0.01$.

tions into the PPRE. The increases in PPARα promoter activity by the ligands were all diminished in the PPARα (−/−) cells. Interestingly, fenofibrate retained the positive effect on activity, although somewhat reduced while this effect was lost with LY518674. These results thus show that PPARα is activated by other PPAR subtypes being dependent on LXR.

3.4. LXRE transcriptional assay

Finally, the activity of the luciferase reporter of LXRE was examined in fibroblasts. Fig. 5A shows that the LXR–LXRE-dependent transcription was activated by all the PPAR ligands, and this effect was canceled by down-regulation of the LXRα gene by a specific siRNA in WI38 cells. When this activity was examined in fibroblasts from wild-type and PPARα(−/−) mice, the activation was diminished with all of the ligands tested in the absence of PPARα. The effects of fenofibrate and LY518674 were almost completely reduced (Fig. 5B).

4. Discussion

We investigated the mechanism for increased transcription of the ABCA1 gene upon pretreatment with PPAR ligands including four fibrates, fenofibrate, bezafibrate, gemfibrozil and LY518674 that preferentially activate PPARα, PPARδ-specific GW501516, and PPARγ-selective pioglitazone. All ligands induced increased ABCA1 mRNA and protein along with an elevation in HDL biogenesis by apoA-I in fibroblasts and macrophages, consistent with previous findings. In addition, they increased mRNAs encoding LXRα and LXRβ, and all three PPARs, PPARα, PPARδ and PPARγ. In the absence of PPARα, the effects of fenofibrate and LY518674 on the ABCA1/HDL biogenesis pathway were decreased including activation by the LXRα ligand, suggesting predominant dependency of these fibrates on PPARα. The increase of PPARδ and PPARγ mRNAs was reduced in the absence of PPARα for all of the compounds tested, suggesting their apparent dependence on PPARα. Transcriptional activation of PPARα is, at least, induced by all the compounds in an LXRα-dependent manner. We conclude that activation of PPARs induces transcriptional increase of the genes encoding PPARs and LXRα, and that this induction requires LXRα and PPARα. Fenofibrate and LY518674 have rather narrow specificity to PPARα but the other compounds, notably bezafibrate has a broad specificity among PPAR subtypes, in agreement with previous reports. The present results also suggest parallel effects of PPARδ with other PPAR subtypes in atherogenesis at least with respect to cholesterol transport.

It was previously shown that the increase in ABCA1 expression and HDL biogenesis by Wy1463 and fenofibrate is LXRα-dependent [4,5]. LXRα is activated by oxysterols and its primary function is to maintain cellular cholesterol homeostasis. It is therefore quite relevant that activation of LXRα leads to induction of the genes required for release of cholesterol, such as those encoding ABCA1 and ABCG1 through LXR response element (LXRE) in their proximal promot-

ers [10]. It was also reported that PPARγ directly induces LXRα expression and leads to coupled induction of ABCA1 through a transcriptional cascade and regulates a pathway of cholesterol removal from macrophages [27]. Moreover, a PPARδ agonist, GW501516, reportedly increased the expression of ABCA1 and induced apoA1-mediated cell cholesterol release in macrophages, fibroblasts, and intestinal cells [20]. The present data demonstrated that all the PPAR agonists require LXRα for increased transcription of the ABCA1 gene. However, another PPARδ agonist reportedly promoted lipid accumulation in human macrophages by increasing expression of the class A and class B scavenger receptors (SR-A and CD36) and adipophiline [22].

Interestingly, a requirement of LXRα was demonstrated not only for enhanced ABCA1 gene transcription but also induction of PPARs in this study. Fenofibrate, bezafibrate, gemfibrozil, LY518674, GW501516, and pioglitazone all increased ABCA1 expression and HDL biogenesis in human THP1 macrophages, human fibroblast WI38 cells and primary mouse fibroblasts. All of these compounds also increased LXRα-mRNA and enhanced expression of PPAR isoforms in an LXRα-dependent manner. We therefore examined the PPARα promoter and LXR-LXRE dependent transcriptional activity in human and mouse fibroblasts. The PPARα promoter was activated by all compounds in an LXRα-dependent manner and partially in a PPARα-dependent manner in mouse fibroblast. The former finding is consistent with a recent report by Inoue et al. [28]. LY518674 is more dependent on PPARα in PPARα promoter activation than the other PPARs agonists used in this study. We also demonstrated that LXRE-luciferase activity was enhanced by all compounds in an LXRα-dependent manner and partially in a PPARα-dependent manner in mouse fibroblast, and fenofibrate and LY518674 are more dependent on PPARα in LXRE-luciferase activity. What is puzzling is that the PPARα promoter activity was enhanced by fenofibrate in the PPARα(−/−) cells in the presence of LXRα.

The effects of the PPAR agonists on transcription of the genes encoding ABCA1, LXRs and PPARs were not strictly distinguishable each other. Disruption of PPARα markedly diminished the effects of fenofibrate and LY518674 indicating the narrow specificity of these agonists toward PPARα. Interestingly, the effects of GW501516 and pioglitazone were also substantially diminished by loss of PPARα expression. In addition, the PPARα promoter was activated by these compounds. These findings indicate two possibilities: (1) GW501516 and pioglitazone may activate PPARα in addition to their specific respective targets PPARδ and PPARγ, respectively; (2) PPARδ and PPARγ increase transcription of PPARα via LXRα to exhibit PPARα-dependency as part of their activity. However, we cannot differentiate among these possibilities based on the data presently available.

PPAR and LXR form obligate heterodimers with retinoid X receptor (RXR) (PPAR/RXR, LXR/RXR) and regulate gene transcription. PPARγ but not PPARα or PPARδ activates LXR directly because of the presence of a response element upstream of the LXR promoter region [27]. However, PPARα and LXR negatively regulate their transcription by inhibiting dimerization with RXRs, and by direct interaction with PPAR and LXR [29,30]. In contrast to these reports, all the PPAR ligands increased mRNA encoding LXRs and PPARs and increased LXRE-luciferase activity and PPARα promoter activity in the present study. Therefore, PPARs and LXR are necessary for their activation, either partially or completely.

In this study, we employed the experimental conditions that mostly depend on endogenous PPARs and ABCA1 rather than relying on the use of transfected and overexpressed genes employed in previous studies [4,5,9,30]. Thus the data are hopefully of more physiological relevance. Based on these observations, we conclude that PPARs and LXRα consist of complex networks including activation among PPAR subtypes for regulation of target genes. The effects of PPAR ligands exhibit their effect as a result of these complex signal transduction networks. This information should be beneficial for future development of anti-atherogenic compounds targeting PPARs [18]. The results and discussion above are summarized in Fig. 6.

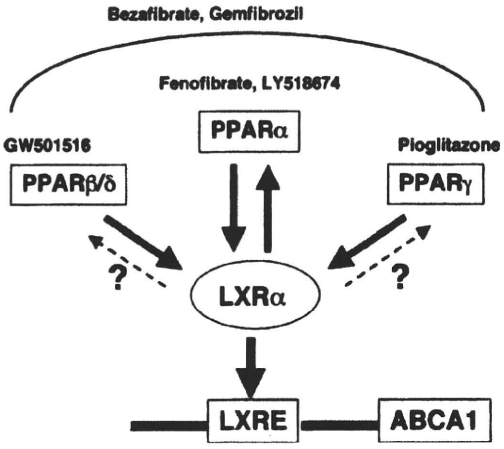

Fig. 6. Summary of the results and discussion. Thick and solid arrows indicate the pathways for transcriptional activation demonstrated in this study. Thin and broken arrows with question marks indicate potential but unproven pathways. Relative selectivity of the fibrates is illustrated as fenofibrate and LY 518674 for PPARα, GW501516 for PPARβ/δ, pioglitazone for PPARγ and bezafibrate and gemfibozil for relatively broad spectrum.

Some questions remain unresolved in this study. Activation of PPARs may induce production of the endogenous ligands for LXRs, and this would contribute to enhancement of transcription of the PPARs and ABCA1 genes in addition to induction of the LXRs gene transcription. Differential effects on the cholesterol and phospholipid release and on cellular ABCA1 protein were observed among the drugs and cell lines (Figs. 1–3A). These findings may be related to unknown cellular factors to regulate cholesterol content in the HDL generated in the ABCA1/apoA-I-dependent HDL biogenesis including subcellular distribution of ABCA1 [31]. Finally, clinical relevance remains to be determined with respect to contribution of transcriptional enhancement of ABCA1 by the mechanism found here to anti-atherogenic effects of PPAR agonists. These questions are to be answered by further investigation of this topic.

Acknowledgments

This work was supported by Grants-in-Aid from the Ministry of Education, Science, Culture and Sports and Technology of Japan and from Japan Health Science Foundation, and by the Program for Promotion of Fundamental Studies in Health Sciences of the National Institute of Biomedical Innovation.

References

[1] Yokoyama S. Assembly of high-density lipoprotein. Arterioscler Thromb Vasc Biol 2006;26:20–7.
[2] Singaraja RR, Brunham LR, Visscher H, Kastelein JJ, Hayden MR. Efflux and atherosclerosis: the clinical and biochemical impact of variations in the ABCA1 gene. Arterioscler Thromb Vasc Biol 2003;23:1322–32.
[3] Staels B, Dallongeville J, Auwerx J, Schoonjans K, Leitersdorf E, Fruchart JC. Mechanism of action of fibrates on lipid and lipoprotein metabolism. Circulation 1998;98:2088–93.
[4] Chinetti G, Lestavel S, Bocher V, et al. PPAR-alpha and PPAR-gamma activators induce cholesterol removal from human macrophage foam cells through stimulation of the ABCA1 pathway. Nat Med 2001;7:53–8.
[5] Arakawa R, Tamehiro N, Nishimaki-Mogami T, Ueda K, Yokoyama S. Fenofibric acid, an active form of fenofibrate, increases apolipoprotein A-I-mediated high-density lipoprotein biogenesis by enhancing transcription of ATP-binding cassette transporter A1 gene in a liver X receptor-dependent manner. Arterioscler Thromb Vasc Biol 2005;25:1193–7.

[6] Cabrero A, Cubero M, Llaverias G, et al. Differential effects of peroxisome proliferator-activated receptor activators on the mRNA levels of genes involved in lipid metabolism in primary human monocyte-derived macrophages. Metabolism 2003;52:652–7.
[7] Peters JM, Aoyama T, Burns AM, Gonzalez FJ. Bezafibrate is a dual ligand for PPARalpha and PPARbeta: studies using null mice. Biochim Biophys Acta 2003;1632:80–9.
[8] Hossain MA, Tsujita M, Gonzalez FJ, Yokoyama S. Effects of fibrate drugs on expression of ABCA1 and HDL biogenesis in hepatocytes. J Cardiovasc Pharmacol 2008;51:258–66.
[9] Sprecher DL, Massien C, Pearce G, et al. Triglyceride: high-density lipoprotein cholesterol effects in healthy subjects administered a peroxisome proliferator activated receptor delta agonist. Arterioscler Thromb Vasc Biol 2007;27:359–65.
[10] Tall AR. Cholesterol efflux pathways and other potential mechanism involved in the athero-protective effect of high density lipoproteins. J Intern Med 2008;263:256–73.
[11] Barter P, Rye KA. Is there a role of fibrate in the management of dyslipidemia in the metabolic syndrome? Arterioscler Thromb Vasc Biol 2008;28:39–46.
[12] Rubins HB, Robins SJ, Collins D, et al. Gemfibrozil for the secondary prevention of coronary heart disease in men with low levels of high-density lipoprotein cholesterol. Veterans Affairs High-Density Lipoprotein Cholesterol Intervention Trial Study Group. N Engl J Med 1999;341:410–8.
[13] Hirakata M, Tozawa R, Imura Y, Sugiyama Y. Comparison of the effects of pioglitazone and rosiglitazone on macrophage foam cell formation. Biochem Biophys Res Commun 2004;323:782–8.
[14] Marx N, Duez H, Fruchart JC, Staels B. Peroxisome proliferator-activated receptors and atherogenesis: regulators of gene expression in vascular cells. Circ Res 2004;94:1168–78.
[15] Tontonoz P, Hu E, Spiegelman BM. Regulation of adipocyte gene expression and differentiation by peroxisome proliferator activated receptor gamma. Curr Opin Genet Dev 1995;5:571–6.
[16] Picard F, Auwerx J. PPAR(gamma) and glucose homeostasis. Annu Rev Nutr 2002;22:167–97.
[17] Li AC, Binder CJ, Gutierrez A, et al. Differential inhibition of macrophage foam-cell formation and atherosclerosis in mice by PPARα, β/δ, and γ. J Clin Invest 2004;114:1564–76.
[18] Staels B, Maes M, Zambon A. Fibrates and future PPARalpha agonists in the treatment of cardiovascular disease. Nat Clin Pract Cardiovasc Med 2008;5:542–53.
[19] Li AC, Glass CK. PPAR- and LXR-dependent pathways controlling lipid metabolism and the development of atherosclerosis. J Lipid Res 2004;45:2161–73.
[20] Oliver Jr WR, Shenk JL, Snaith MR, et al. A selective peroxisome proliferator-activated receptor delta agonist promotes reverse cholesterol transport. Proc Natl Acad Sci USA 2001;98:5306–11.
[21] Lee CH, Chawla A, Urbiztondo N, et al. Transcriptional repression of atherogenic inflammation: modulation by PPARdelta. Science 2003;302:453–7.
[22] Vosper H, Patel L, Graham TL, et al. The peroxisome proliferator-activated receptor delta promotes lipid accumulation in human macrophages. J Biol Chem 2001;276:44258–65.
[23] Lee SS, Pineau T, Drago J, et al. Targeted disruption of the alpha isoform of the peroxisome proliferator-activated receptor gene in mice results in abolishment of the pleiotropic effects of peroxisome proliferators. Mol Cell Biol 1995;15:3012–22.
[24] Xu Y, Mayhugh D, Saeed A, et al. Design and synthesis of a potent and selective triazolone-based peroxisome proliferator-activated receptor alpha agonist. J Med Chem 2003;46:5121–4.
[25] Pineda Torra I, Jamshidi Y, Flavell DM, Fruchart JC, Staels B. Characterization of the human PPARalpha promoter: identification of a functional nuclear receptor response element. Mol Endocrinol 2002;16:1013–28.
[26] Suzuki S, Nishimaki-Mogami T, Tamehiro N, et al. Verapamil increases the apolipoprotein-mediated release of cellular cholesterol by induction of ABCA1 expression via Liver X receptor-independent mechanism. Arterioscler Thromb Vasc Biol 2004;24:519–25.
[27] Chawla A, Boisvert WA, Lee CH, et al. A PPAR gamma-LXR-ABCA1 pathway in macrophages is involved in cholesterol efflux and atherogenesis. Mol Cell 2001;7:161–71.
[28] Inoue J, Satoh S, Kita M, et al. PPARalpha gene expression is up-regulated by LXR and PXR activators in the small intestine. Biochem Biophys Res Commun 2008;371:675–8.
[29] Yoshikawa T, Ide T, Shimano H, et al. Cross-talk between peroxisome proliferator-activated receptor (PPAR) alpha and liver X receptor (LXR) in nutritional regulation of fatty acid metabolism. I. PPARs suppress sterol regulatory element binding protein-1c promoter through inhibition of LXR signalling. Mol Endocrinol 2003;17:1240–54.
[30] Ide T, Shimano H, Yoshikawa T, et al. Cross-talk between peroxisome proliferator-activated receptor (PPAR) alpha and liver X receptor (LXR) in nutritional regulation of fatty acid metabolism. II. LXRs suppress lipid degradation gene promoters through inhibition of PPAR signalling. Mol Endocrinol 2003;17:1255–67.
[31] Lu R, Arakawa R, Ito-Osumi C, Iwamoto N, Yokoyama S. ApoA-I facilitates ABCA1 recycle/accumulation to cell surface by inhibiting its intracellular degradation and increases HDL generation. Arterioscler Thromb Vasc Biol 2008;28:2282–7.

JOURNAL OF LIPID RESEARCH

FGF-1 induces expression of LXRα and production of 25-hydroxycholesterol to upregulate the apoE gene in rat astrocytes

Rui Lu,* Jinichi Ito,* Noriyuki Iwamoto,* Tomoko Nishimaki-Mogami,† and Shinji Yokoyama[1,*]

Department of Biochemistry,* Nagoya City University Graduate School of Medical Sciences, Nagoya 467-8601, Japan; and Department of Biochemistry and Metabolism,† National Institute of Health Sciences, Tokyo 158-8501, Japan

Abstract **Fibroblast growth factor 1 (FGF-1) enhances apolipoprotein E (apoE) expression and apoE-HDL biogenesis in autocrine fashion in astrocytes (Ito, J., Y. Nagayasu, R. Lu, A. Kheirollah, M. Hayashi, and S. Yokoyama. Astrocytes produce and secrete FGF-1, which promotes the production of apoE-HDL in a manner of autocrine action. *J. Lipid Res.* 2005. 46: 679–686) associated with healing of brain injury (Tada,T., J-i. Ito, M. Asai, and S. Yokoyama. Fibroblast growth factor 1 is produced prior to apolipoprotein E in the astrocytes after cryo-injury of mouse brain. *Neurochem. Int.* 2004. 45: 23–30). FGF-1 stimulates mitogen-activated protein kinase kinase/extracellular signal-regulated kinase (MEK/ERK) to increase cholesterol biosynthesis and phosphatidylinositol 3-OH kinase (PI3K)/Akt to enhance apoE-HDL secretion (Ito, J., Y. Nagayasu, K. Okumura-Noji, R. Lu, T. Nishida, Y. Miura, K. Asai, A. Kheirollah, S. Nakaya, and S. Yokoyama. Mechanism for FGF-1 to regulate biogenesis of apoE-HDL in astrocytes. *J. Lipid Res.* 2007. 48: 2020–2027). We investigated the mechanism for FGF-1 to upregulate apoE transcription. FGF-1 increased apoE and liver X receptor α (LXRα) mRNAs in rat astrocytes. Increase of LXRα mRNA was suppressed by inhibition of the FGF-1 receptor-1 and MEK/ERK but not by inhibition of PI3K/Akt. The increases of apoE mRNA and apoE-HDL secretion were both inhibited by downregulation or inhibition of LXRα, while they were partially suppressed by inhibiting cholesterol biosynthesis. We identified the liver X receptor element responsible for activation of the rat apoE promoter by FGF-1 located between −450 and −320 bp, and the direct repeat 4 (DR4) element in this region (−448 to −433 bp) was responsible for the activation. Chromatin immunoprecipitation analysis supported that FGF-1 enhanced association of LXR with the rat apoE promoter. FGF-1 partially activated the apoE promoter even in the presence of an MEK inhibitor that inhibits the FGF-1-mediated enhancement of cholesterol biosynthesis. On the other hand, FGF-1 induced production of 25-hydroxycholesterol by MEK/ERK as an sterol regulatory element-dependent reaction besides cholesterol biosynthesis. We concluded that FGF-1-induced apoE expression in astrocytes depends on LXRα being mediated by both LXRα expression and an LXRα ligand biosynthesis.**—Lu, R., J. Ito, N. Iwamoto, T. Nishimaki-Mogami, and S. Yokoyama. **FGF-1 induces expression of LXRα and production of 25-hydroxycholesterol to upregulate the apoE gene in rat astrocytes.** *J. Lipid Res.* **2009.** 50: **1156–1164.**

Supplementary key words high density lipoprotein • cholesterol • direct repeat 4

Apolipoprotein E (apoE) is a glycoprotein composed of 299 amino acids and plays critical roles in lipid metabolism. While most of apolipoproteins are synthesized and secreted primarily by the liver and intestine, apoE is in addition secreted by other cells outside the enterohepatic axis, such as macrophages and adipocytes (1, 2). ApoE is also synthesized by astrocytes and microglia in the central nervous system (CNS) and forms HDL as a major lipoprotein in CNS (3, 4). CNS is segregated from systemic circulation by the blood brain barrier and prevented from access to plasma lipoproteins, so that HDL generated in CNS is the exclusive lipid transport system among the CNS cells (5). ApoE-HDL plays many key roles in maintaining integrity and regeneration of CNS by mediating intercellular lipid transport. ApoE synthesis in glia cells increases during development and after injury of CNS (6–11).

We demonstrated that absence of apoE delayed healing of cryo-injury of mouse brain, as evidenced by expression

This study was supported by International HDL Award Program, in part by grants-in-aid from The Ministries of Education, Science, Technology, Culture, and Sports, and of Health, Welfare, and Labor of Japan, and by the Program for Promotion of Fundamental Studies in Health Sciences of National Institute of Biomedical Innovation. Rui Lu is supported by Postdoctoral Fellowship for Foreign Researchers from the Japan Society for the Promotion of Science.

Manuscript received 17 November 2008 and in revised form 12 December 2008 and in re-revised form 18 February 2009.

Published, JLR Papers in Press, February 19, 2009.
DOI 10.1194/jlr.M800594-JLR200

Abbreviations: apoE, apolipoprotein E; ChIP, chromatin immunoprecipitation; CNS, central nervous system; ERK, extracellular signal-regulated kinase; FGF, fibroblast growth factor; FGFR1, FGF receptor 1; LXR, liver X receptor; LXRE, LXR response element; MEK, mitogen-activated protein kinase kinase; ERK, extracellular signal-regulated kinase; PI3K, phosphatidylinositol 3-OH kinase; siRNA, small interfering RNA; SRE, sterol regulatory element; TK, thymidine kinase.

[1] To whom correspondence should be addressed.
e-mail: syokoyam@med.nagoya-cul.ac.jp

of fibroblast growth factor 1 (FGF-1) and subsequent apoE expression in the astrocytes in the peri-injury regions (12). Long-term culture of rat astrocytes induced the increase of apoE synthesis and apoE-HDL production and enhancement of cholesterol biosynthesis, in comparison to the astrocytes prepared by a conventional method of 1-week primary and 1-week secondary culture (13). FGF-1 was highly expressed and released in these long-cultured cells, and their conditioned medium and FGF-1 both stimulated apoE synthesis, production of apoE-HDL, and cholesterol biosynthesis in the conventionally prepared astrocytes (14).

FGF-1 was shown in astrocytes to activate the mitogen-activated protein kinase kinase/extracellular signal-regulated kinase (MEK/ERK) signaling pathway for the increase of cholesterol biosynthesis and the phosphatidylinositide 3-OH kinase (PI3K)/Akt pathway to enhance secretion of apoE/apoE-HDL, being mediated by the receptor (15). It also stimulated transcription of the apoE gene mediated by the receptor, but with an unknown pathway (15). To understand the mechanism for FGF-1 to stimulate astrocytes for biogenesis of apoE-HDL in response to brain injury and to expedite its healing process, we further investigated the mechanism for FGF-1 to increase transcription of apoE in astrocytes. FGF-1 was shown to enhance apoE transcription through the increase of interaction of the liver X receptor (LXR)α, a nuclear receptor for oxysterol being involved in sterol homeostasis, with a conserved direct repeat 4 (DR4) sequence in LXR response element (LXRE) present in the apoE promoter. This reaction was mediated by the increase of LXRα expression and by the production of its ligand.

MATERIALS AND METHODS

Cell Culture

Astrocytes were prepared from 17-day fetal brain of Wistar rats according to the method previously described (16). The brain cells were cultured in F-10 medium (GIBCO) containing 10% (v/v) fetal calf serum for 1 week as primary culture and for subsequent 1 week as secondary culture. Fibroblasts of BALB/3T3 mouse were obtained from the RIKEN cell bank. The cells were cultured in DF medium (1:1 mixture of DMEM and Ham's F12 medium) with 10% (v/v) fetal calf serum.

RNA Isolation and real-time PCR analysis

Total RNA was isolated from the cells using an ISOGEN kit (Nippon Gene). Real-time PCR analysis was performed on an ABI PRISM 7700 sequence detection system using target-specific probes. Those for apoE and LXRα were described elsewhere (14, 17). For HMG-CoA reductase, SREBP2, cholesterol 24-hydroxylase (CYP46A1), and cholesterol 25-hydroxylase, the probes chosen were 5′-TGCTGCTTTGGCTGTATGTC-3′ and 5′-TGAGCGTGAACAAGAACCAG-3′, 5′-CCAAGAAGAAGGCAGGTGAC-3′ and 5′-GGACCCGCTCTACTTCAGTG-3′, 5′-GTGACTATGGGCGCTGGTAT-3′ and 5′-ATCAGCTGCTCTGCCTTCTC-3′, and 5′-TAGCCTTCTTGGATGTGCTG-3′and 5′-GTGAGTGGACCACGGAAAGT-3′, respectively.

Western blot analysis

Cell lysates or media concentrates (concentrated using the BCA Protein Assay Kit; Pierce) were subjected to 10% SDS-PAGE (50 μg protein/lane) and then transferred to a polyvinylidene difluoride membrane. Bands of apoE were visualized by using the specific antibody (Santa Cruz Biotechnology). Intensity of photoimage was digitalized by scanning using an EPSON GT-X700 and analyzed with Adobe Photoshop software for quantification.

RNA interference

Small interfering RNA (siRNA) specific primers for rat LXRα and a scramble control were obtained from Invitrogen and transfected into rat primary astrocytes using Lipofectamine 2000 (Invitrogen) according to the manufacturer's protocol.

Construction of luciferase reporter genes and luciferaase assay

The promoter region of rat apoE gene was prepared by PCR using rat normal liver genomic DNA (18) as a template using primers tailed with *KpnI* and *XhoI* (New England Biolabs). Each PCR product was ligated into *KpnI*/*XhoI* sites of PGVB Basic vector and confirmed by sequencing. Six reporter gene constructs were assembled with the segments of the apoE promoter from −690, −600, −450, −320, −200, and −135 bp to +9 bp. To obtain a reporter construct with mutation of apoE DR4 element (DR4mu), site-directed mutagenesis was performed to introduce the DR4 at −448 to −433 bp of the −690 to +9 reporter gene using a Quick Change II Site-Directed Mutagenesis Kit (Stratagene, La Jolla, CA) and the respective primers, DR4 of forward: 5′-CCGGGGATGGGGAGttaaCACCGTGGCAGAGGAATCACTA-3′, reverse: 5′-TAGTGATTCCTCTGCCACGGTGttaaCTCCCCATCCCCGG-3′ (lowercase letters indicate mutated nucleotides). The plasmid for expression of LXRα and the reporter plasmid containing four tandem repeats of LXREs upstream of the thymidine kinase (TK) promoter and its mutant, LXRE-TK and LXREmut-TK, the promoter plasmid containing sterol regulatory element (SRE), were prepared as previously described (19, 20). 3T3 cells were grown to 60–70% confluence in 24-well plates, transfected with 1 μg of plasmid DNA including 0.2 μg LXRα expression vector, 0.77 μg reporter gene construct, and 30 ng hRluc-TK (Promega; for normalization) using Lipofectamine 2000 (Invitrogen). The luciferase activity was measured using a Dual-Luciferase Reporter System (Promega).

Chromatin immunoprecipitation analysis

Chromatin immunoprecipitation (ChIP) assay was conducted as previously described (20). Briefly, rat primary astrocytes were fixed with 1% formaldehyde. Cross-linked adducts were resuspended and sonicated to yield DNA fragments of 200 to 1,200 bp. Immunoprecipitation was performed using anti-LXRα antibody (Perceus Proteomics). Mouse normal IgG (Santa Cruz Biotechnology) was used as a control for nonspecific binding. Protein-bound, immunoprecipitated DNA was reverse cross-linked at 65°C overnight and then purified using a PCR purification Kit (Sigma-Aldrich). Ten microliters from a 50-μl DNA extraction volume was used for PCR amplification (33 cycles). The set of primers forward, 5′-CAGAGCTAACAAGTAACACA-3′, and reverse, 5′-AAAAGGGCTGGAGGCTTAAA-3′, was used to amplify the region on the promoter of the apoE gene.

Analysis of cholesterol biosynthesis and oxysterol production

Cholesterol biosynthesis in astrocytes was estimated by incubating astrocytes with ^{3}H-acetate as described elsewhere (15). Lipid was extracted from the cells and analyzed by TLC. For evaluation of production of 25-hydroxycholesterol, the cells were labeled with ^{14}C-cholesterol conjugated with 2% cyclodextrin for 30 min at 37°C, washed with PBS three times, and incubated in 0.1% BSA-F-10 in the presence of FGF-1, U0126, or compactin for 16 h.

JOURNAL OF LIPID RESEARCH ASBMB

Lipid was extracted and analyzed by TLC to detect the count in 25-hydroxycholesterol. Efficacy of the lipid extraction procedure (16) was 88 ± 5% estimated by the recovery of ^{14}C-cholesterol exogenously added.

Other Reagents

FGF-1, TO901317 (an LXR agonist), PD173074, LY294002, and U1026 (inhibitors of the FGF receptor 1 (FGFR1), PI3K, and MEK1/2, respectively) were all purchased from Sigma-Aldrich. SB203580 and SP600125, inhibitors of P38 mitogen-activated protein kinase and stress-activated protein kinase/c-Jun NH2-terminal kinase, respectively, were also obtained from Sigma-Aldrich.

RESULTS

Astrocytes were stimulated by FGF-1 at a confluent stage, and the levels of mRNA were measured for LXRα and apoE in time-dependent manners (**Fig. 1A**). The both messages increased by the FGF-1 treatment up to 12 h in parallel, by 3.5-fold for LXRα and by 7.5-fold for apoE mRNA. LXRα mRNA further increased at least for 24 h by the incubation, while apoE mRNA reached plateau at 12 h. FGF-1 enhanced expression of ABCA1 mRNA being consistent with the increase of LXRα but did not influence expression of LXRβ (Fig. 1B). Fig. 1C shows the increases of apoE mRNA and LXRα mRNA expressions by FGF-1 and their almost complete suppression by an FGFR1 inhibitor PD173074. An MEK/ERK pathway inhibitor, U0126, partially suppressed expression of apoE and LXRα mRNAs. The inhibition beyond the level of control without exogenous FGF-1 may indicate the presence of the basal autocrine activation by endogenous FGF-1 (14). A PI3K/Akt pathway inhibitor LY294002 that inhibits apoE secretion (15) did not influence the expression of either mRNA.

As the apoE gene transcription was reportedly regulated by LXRs (21, 22), we examined whether the FGF-1-induced expression of apoE depends on LXR. Rat astrocytes were transfected with LXRα siRNA to reduce its mRNA expression by 80% and examined for the reactivity of apoE expression by FGF-1. Expression of apoE was reduced by the siRNA treatment estimated as the mRNA and protein level, regardless of the presence of FGF-1, and this was reflected by the decrease in cellular and secreted apoE protein (**Fig. 2A**). Dependency of the FGF-1-induced apoE expression on LXR was also demonstrated by inhibition of LXR by arachidonic acid, a competitive but not highly specific inhibitor of LXRα (23), shown as a decrease of cellular and secreted apoE (Fig. 2B). LXRα is activated by oxysterol that generally increases in parallel with cellular cholesterol, so that the effect of inhibition of cholesterol biosynthesis was examined. The cells were treated with compactin, an HMG-CoA reductase inhibitor, and the FGF-1-induced increase of LXRα mRNA was decreased by overall 62% (85% of the increase by exogenous FGF-1) and that of apoE mRNA was by 74% (**Fig. 3**). Thus, upregulation of the apoE gene transcription in astrocytes is associated with the increase of LXRα, both being regulated by cellular sterol biosynthesis.

To investigate molecular mechanism for FGF-1 to upregulate apoE expression, the promoter of the apoE gene

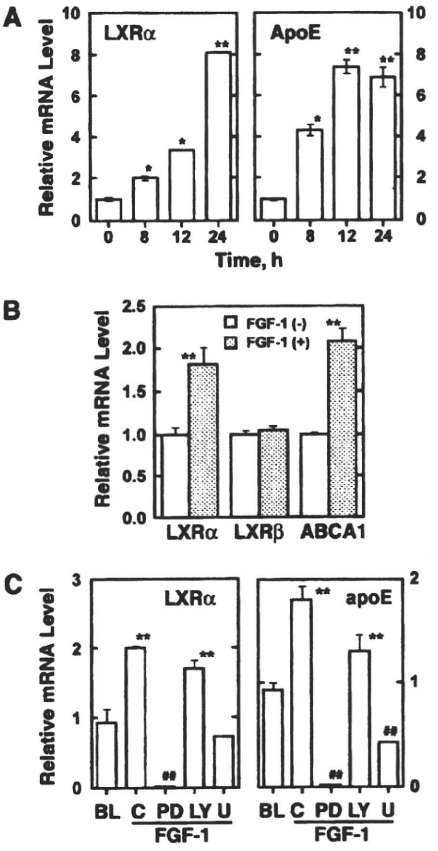

Fig. 1. A: Increase of expression of LXRα and apoE by FGF-1 in rat astrocytes. Primary astrocytes at a confluent stage were treated with 50 ng/ml FGF-1 for the indicated times, and mRNA of LXRα and apoE was determined by real time-PCR. The data are standardized for β-actin and expressed as relative increase to the cells incubated without FGF-1 as controls. B: Effects of FGF-1 on expression of ABCA1 and LXRβ. Experiments were performed as described above with incubation of the cells with FGF-1 for 8 h. C: Induction of mRNA of LXRα and apoE in rat astrocytes. Rat astrocytes in primary culture were treated with FGF-1 in the presence of 10 μM PD173074 (PD), LY294002 (LY), U1026 (U), inhibitors of FGFR1, PI3K, and MEK, respectively. The messages for LXRα and apoE were quantified by real-time PCR as described as above. Data represent the average ± SD of three measurements (some SD values may be too small to appear in the graph). * $P < 0.05$ and ** $P < 0.01$ increase from control. ## $P < 0.01$ decrease from control.

was analyzed by using luciferase reporter assay. Six reporter genes were constructed to find a specific region(s) responsible for the FGF-1 induced activation, between −690 and +9 bp of the apoE promoter, −600 and 9 bp, −450 and +9 bp, −320and 9 bp, −200 bp and 9 bp, and −135 bp and +9 bp (**Fig. 4A**). The activity of the reporter genes was examined for the response to the FGF-1 treatment as well as to an LXR agonist, TO901317, in the transiently transfected 3T3 cells under overexpression of LXRα. As shown in Fig. 4B, FGF-1 and TO901317 activated the reporter genes as far as they contain the region −450 bp or its upstream, and this response was lost with the gene of −320 bp. We thus assumed

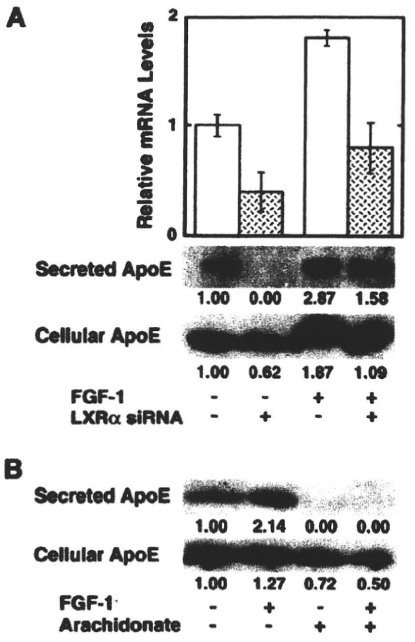

Fig. 2. Effects of inhibition of LXRα expression or of its activation on expression of apoE mRNA and its secretion in astrocytes. A: Rat primary astrocytes were transfected with 20 nM LXRα siRNA and control siRNA as described in the text to suppress its expression. After the 72-h transfection, the cells were treated with 50 ng/ml FGF-1 for 16 h. apoE mRNA and cellular apoE protein at 16 h and apoE secreted into the medium during 16 h were determined by real-time PCR and by Western blotting, respectively. The data are expressed as relative to those by a control scrambled siRNA. B: Rat astrocytes were incubated with 100 μM arachidonate for 16 h to inhibit LXR activity before the treatment with 50 ng/ml FGF-1 for 16 h in the presence of arachidonate. Cellular and secreted apoE were estimated by Western blotting. Data represents the average ± SD of three measurements. * $P < 0.05$ to siRNA (−). Numbers indicate density of the bands relative to control.

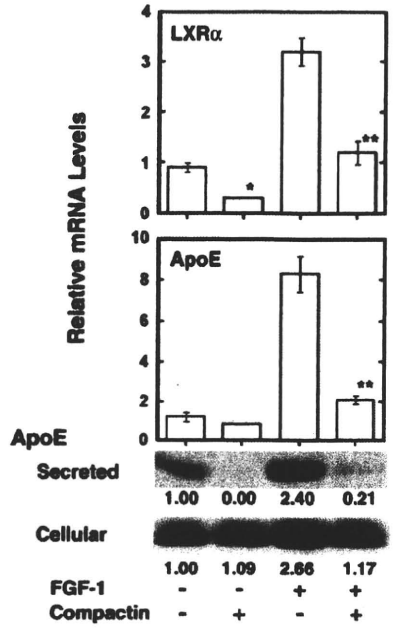

Fig. 3. Effects of inhibition of cholesterol biosynthesis on the increase of expression of LXRα and apoE, as well as on secretion of apoE. Rat primary astrocytes were pretreated with 5 μM compactin for 2 h, and the cells were treated with 50 ng/ml FGF-1 for 16 h. Expression of mRNA of apoE and LXRα was determined by real-time PCR, and cellular and secreted apoE were analyzed by Western blotting. Data represent the average ± SD of three measurements. * $P < 0.05$ and ** $P < 0.01$ to compactin (−). Numbers indicate density of the bands relative to control.

that the region between −450 and −320 bp is responsible for activation by LXR and FGF-1. DR4 sequence was identified as AGTTCACCGTGGCAGA (−448 to −433 bp) in this region, so that mutation was introduced to this sequence as TTAACACCGTGGCAGA of the −600 to +9 bp construct (LXREmut) (Fig. 4A), and its activity was examined. Responses of the reporter genes to FGF-1 and to TO901317 both disappeared by introducing this mutation (Fig. 4C). To confirm that this sequence is generally responsible for activation by FGF-1, the reporter genes were constructed with the heterologous promoter of TK that contains the same DR4 sequence. The promoter was activated by FGF-1, and activation was abolished by introducing mutation into the DR4 in this assay system (Fig. 4D). Treatment of the cells of the reporter assay system with an LXR antagonist, arachidonate, decreased the activation by FGF-1 (Fig. 4E) and so did compactin (data not shown). We concluded from these results that one LXRE exit of −448 to −433 bp of the apoE promoter is responsible for increase of the apoE gene transcription by FGF-1 being dependent on LXR.

To confirm that FGF-1 enhances association of LXR with LXRE of the endogenous apoE promoter in astrocytes, ChIP assay was performed in rat primary astrocytes using specific antibody against rat LXRα (**Fig. 5**). Increase of the association was demonstrated by an LXR agonist TO901317 as well as by FGF-1.

The experiments above demonstrated that FGF-1 activates LXR to enhance expression of the apoE gene through its interaction with the LXRE. **Figure 6** demonstrates production of LXR ligands by FGF-1. Cholesterol biosynthesis is increased by FGF-1 (Fig. 6A) in association with increase of expression of the HMG-CoA reductase gene (Fig. 6B). This increase seems to be mediated by activation of the SRE and SRE binding protein system because FGF-1 activated the SRE-luciferase assay system (Fig. 6C). Cholesterol 25-hydroxylase is known to be activated by the SRE system (24), and its expression was indeed increased by FGF-1 and by compactin to a less extent, while expression of cholesterol 24-hydroxylase that is regulated by LXR (24) was not significantly increased by FGF-1 (Fig. 6D, E). Consequently, production of 25-hydroxycholesterol was increased by FGF-1 in astrocytes (Fig. 6F). These effects of FGF-1 were all blocked by an inhibitor of the MEK/ERK pathway, U0126. Thus, FGF-1 at least increases a ligand of LXR, 25-hydroxycholesterol, for the enhancement of the apoE gene expression.

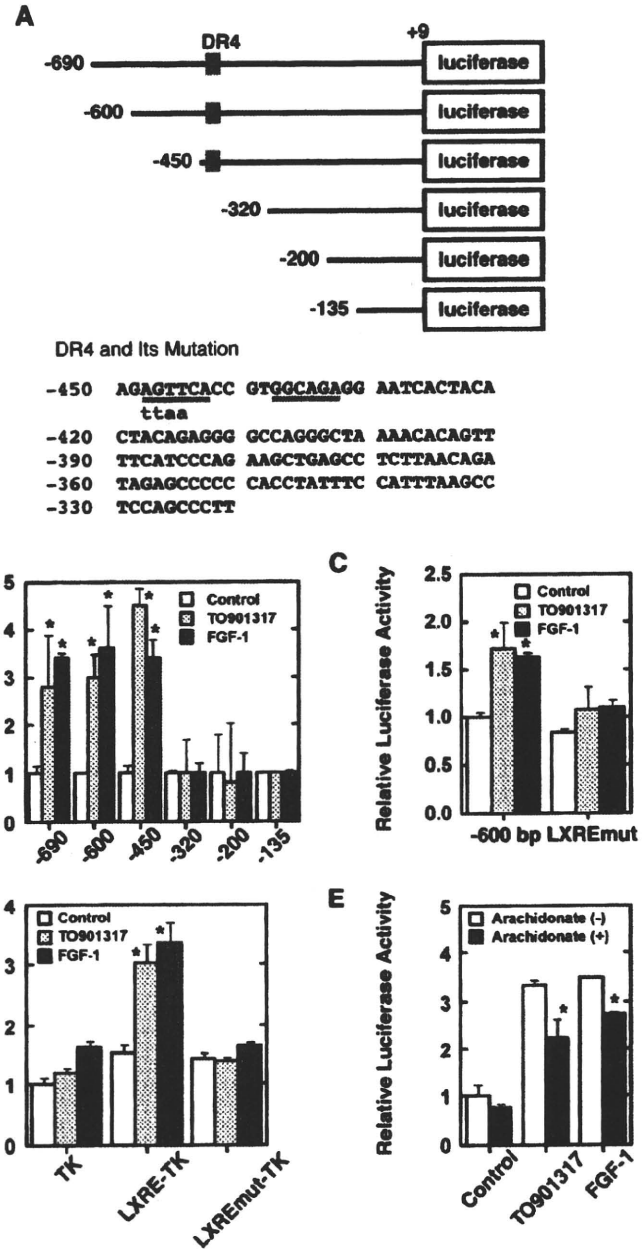

Fig. 4. The results of the reporter gene assays to identify the element responsible for activation by FGF-1 in the apoE promoter or in the heterologous TK promoter that contains 4 × DR4s. The reporter gene constructs were cotransfected with the expression vector for LXRα in 3T3 cells. After 24-h transfection, the cells were incubated with 50 ng/ml FGF-1 or 5 μM T0901317, an agonist for LXRα for 16 h. A: Diagram of the reporter gene constructs for the rat apoE promoter. Numbers indicate of the nucleotide positions, and location of DR4 sequence is indicated by gray boxes. Nucleotide sequence of the segment that contains DR4 and mutations introduced are indicated as lowercase letters for the corresponding nucleotide positions. B: The results with the apoE promoter constructs with various lengths as listed in A. The baseline activity of each reporter gene was 1.22 for −600 bp, 0.72 for −450 bp, 1.44 for −320 bp, 1.67 for −200 bp, and 1.46 for −135 bp, relative to that of −600 bp, respectively. C: The apoE promoter construct of −600 bp and its DR4 mutant (LXREmut) defined in Fig. 4A were used in luciferase assay with TO901317 and FGF-1. D: The results with the TK promoter and its mutant genes, by activation with TO901317 and FGF-1. E: The effects of an LXRα inhibitor, arachidonate, on activation by TO901317 and FGF-1 of the apoE promoter construct of −600 bp. Incubation was carried out as described in the text. Data represent the average ± SD of three measurements/samples. * $P < 0.01$ to the respective control.

We previously demonstrated that FGF-1 enhanced the apoE gene transcription even in the conditions that either the MEK/ERK or PI3K/Akt pathway was inhibited, for enhancement of cholesterol biosynthesis or activation of apoE secretion, respectively (15). The response of the apoE gene promoter to FGF-1 was therefore examined in the presence of those inhibitors to evaluate whether activation of the apoE gene transcription is independent of the related signaling pathways.

The response of the reporter genes to FGF-1 was examined in the presence of an FGFR1 inhibitor, PD173074, a PI3K/Akt pathway inhibitor, LY294002, or an MEK/ERK pathway inhibitor, U0126. The effect of FGF-1 on expression of the gene of −450 bp was abolished by inhibition of FGFR1. Inhibition of the PI3K/Akt pathway did not influence the affect of FGF-1. On the other hand, inhibition of the MEK/ERK pathway by U0126 partially suppressed the effect of FGF-1 (**Fig. 7A**) in the concentration for complete suppression of cholesterol biosynthesis (data not shown), being consistent with the findings in Fig. 1C that induction of LXRα mRNA by FGF-1 was not influenced by inhibition of either signaling pathway. These responses disappeared when the segment between −450 and −320 bp was deleted (Fig. 7B). Thus, we concluded that enhancement of the

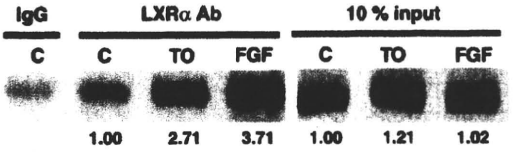

Fig. 5. ChIP analysis for LXRα binding to the apoE promoter. Rat primary culture astrocytes were treated with TO901317 or FGF-1. ChIP analysis was performed with an anti-LXRα antibody and control normal mouse IgG. Primers specific to the LXRE-containing regions of apoE promoter were used for PCR analysis as described in the text. C, control; TO, TO901317; FGF, FGF-1. Numbers indicate density of the bands relative to control.

apoE gene transcription by FGF-1 is dependent on LXRα. The enhancement of the apoE gene transcription seems partially induced by the increase of biosynthesis of the LXRα ligand by FGF-1, but a substantial part may be dependent on the increase of the LXRα expression.

DISCUSSION

apoE is the major endogenous apolipoprotein in CNS, synthesized and secreted by astrocytes and microglias to form apoE-HDL (5). Production of apoE and perhaps apoE-HDL increases in response to acute and chronic damage of CNS, and this seems to play a role in regeneration of nerve cells and healing of the injury. Therefore, it is important to understand the background molecular mechanism for this reaction to understand the process of the recovery of the brain damage. We discovered that apoE-HDL production is stimulated by FGF-1 in astrocytes by an autocrine mechanism and helps the healing process of the brain cryo-injury (12–14). FGF-1 was shown to activate the MEK/ERK signaling pathway to stimulate cholesterol biosynthesis and the PI3K/Ark pathway for enhancement of apoE-HDL secretion (15). It also increases transcription of the apoE gene, but involvement of these pathways is unclear in this reaction (15).

Upregulation of the apoE gene expression was found associated with cellular cholesterol content (25), but the background molecular mechanism for this regulation has not been identified. Two enhancers were identified in the downstream of the human apoE gene, multienhancer 1 and multienhancer 2, that are required for upregulation by sterol and directed macrophage- and adipose-specific expression in transgenic mice (26). The nuclear receptors LXRα and LXRβ and their oxysterol ligands were found to regulate the apoE gene expression by associating LXRE in these enhancers in both macrophages and adipose tissues (21). Thus, the LXR/RXR system is thought to be the major regulatory pathway for apoE gene expression.

LXRs are expressed in CNS (22), and genetic defect of these receptors results in various CNS disorders, such as lipid accumulation, astrocyte proliferation, and disorganization of myelin sheath (27). The LXR/RXR system has also been shown to regulate the apoE gene expression in

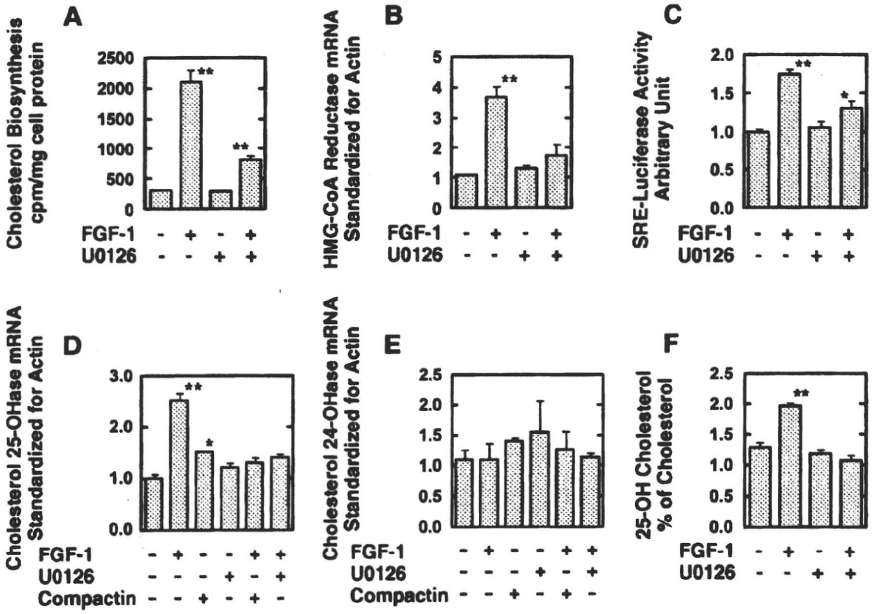

Fig. 6. The effects of FGF-1 to increase cholesterol biosynthesis and production of 25-hydroxycholesterol. A: The effect of FGF-1 and of an inhibitor of the MEK/ERK pathway, U0126. B: Increase of HMG-CoA reductase message and its inhibition by U0126. C: Increase of the SRE reporter gene activity by FGF-1. D: Increase of cholesterol 25-hydroxylase mRNA by FGF-1. The increase by compactin was significant. E: The effects of FGF-1 on cholesterol 24-hydroxylase mRNA. F: Production of 25-hydroxycholesterol. ** $P <$ 0.01 and * $P < 0.05$, respectively.

JOURNAL OF LIPID RESEARCH ASBMB

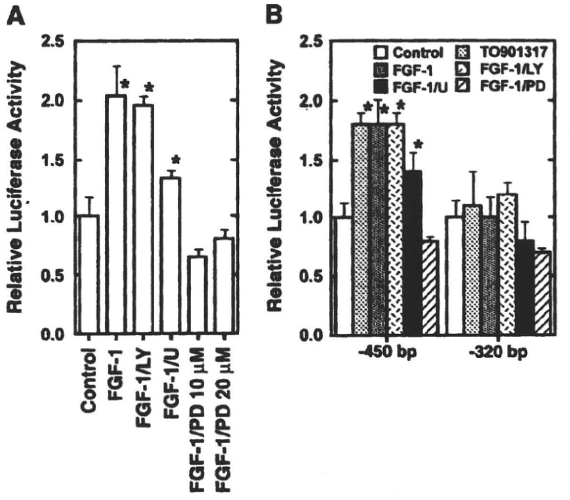

Fig. 7. The effect of inhibitors for FGFR1, the MEK/ERK pathway, and the PI3K/Akt pathway on the reactions induced by 50 ng/ml FGF-1. A: The effects of the inhibitors on the reporter gene expression. The promoter construct of 450 bp was used to investigate contribution of FGFR1 and signaling pathways of MEK/ERK and PI3K to the FGF-1-induced activation of the apoE promoter. The cells were incubated with FGF-1 in the presence of the inhibitors of PI3K, MEK, and FGFR1, as 10 μM of LY294002 (LY) and U1026 (U), and 10 and 20 μM of PD173074 (PD), respectively. B: The effect of the inhibitors on the reporter gene expression. The promoter constructs of 450 and 320 bp were used to confirm that LXRE is responsible for the FGF-1-induced activity and its inhibition. Concentration of TO901317 was 5 μM, and that of the inhibitors was same as above. Data represent the average ± SD of three measurements. * $P < 0.05$ to the respective control.

CNS and to be involved in regulation of cholesterol homeostasis there (28). An LXR ligand, 24(*S*)-hydroxycholesterol and its agonist TO901317, induce LXR-dependent genes, such as apoE, ABCA1, and ABCG1 in astrocytes in vitro (28, 29), but the effect of the latter compound in vivo on apoE expression may not be consistent (30, 31).

FGF-1 is a potent mitogen and growth stimulator that belongs to a family of polypeptide growth factors (32) and stimulates cells through the high affinity tyrosine kinase-linked FGF receptors (FGFR1-4) for their growth, differentiation, and inflammatory reactions (33–35). However, action and behavior of FGF-1 may not be those of typical cytokines that are secreted and react with target cells by inducing intracellular signals. It does not have a signal peptide, synthesized and located in cytosol (36), so that its release from cells is mediated by an unknown mechanism (37). It has a nuclear translocational sequence, and deletion of this domain results in loss of stimulation of DNA synthesis but not induction of signals (38). The effect of FGF-1 on transcription of the apoE gene apparently depends on FGFR-1 and LXR but not on stimulation of the PI3K/Akt pathway and partially on the MEK/ERK pathway to stimulate sterol biosynthesis. Thus, FGF-1 may act to stimulate the LXRα transcriptional activity by direct action of FGF-1 if it could be internalized by FGFR1.

In this article, we investigated the mechanism for FGF-1 to activate expression of the apoE gene. We demonstrated that the promoter of rat apoE gene contains DR4 sequence at the position of −448 to −433 bp, which is responsible for LXRα binding and transcriptional activation of the gene by FGF-1. This DR4 element had homology to the apoE promoter sequence −2590 to −2572 bp of human by 62.5%, and −1439 to −1424 bp and −405 to 389 bp of mouse by 66 and 82%. Functions of these segments are unknown for regulation of the apoE gene. On the other hand, the enhancer DR4 sequence reported by other authors did not match the promoter sequence in this work (21). One multienhancer having DR4 was identified in association with the mouse apoE gene at the corresponding position to human multienhancer 1 with respect to its position (39), and analysis of the rat apoE gene revealed the presence of multienhancer with DR4 in the similar region. Contribution of this DR4 to regulation of the rat apoE gene should be investigated.

It was also demonstrated that transcriptional activation of the apoE gene apparently requires basic level of cholesterol biosynthesis activity in the cells, and inhibition of the increase of cholesterol biosynthesis by FGF-1 may result in its partial decrease, showing that activation of LXR perhaps by oxysterol is a part of the mechanism for this FGF-induced reaction. This view was strongly supported by the findings that FGF-1 induced expression of cholesterol 25-hydroxylase to produce 25-hydroxycholesterol. It is interesting that FGF-1 seems to activate the SRE binding protein pathways to increase cholesterol biosynthesis and therefore activate cholesterol 25-hydroxylase but not cholesterol 24-hydroxylase (24). The effects of compactin on these enzymes also seem consistent with this mechanism. The increase of 25-hydroxycholesterol should activate LXRα and increase apoE transcription. It is interesting that cholesterol 24-hydroxylase transcription was not activated despite the LXR activation, perhaps being consistent with the findings that this enzyme is expressed predominantly in neurons in the brain (40, 41).

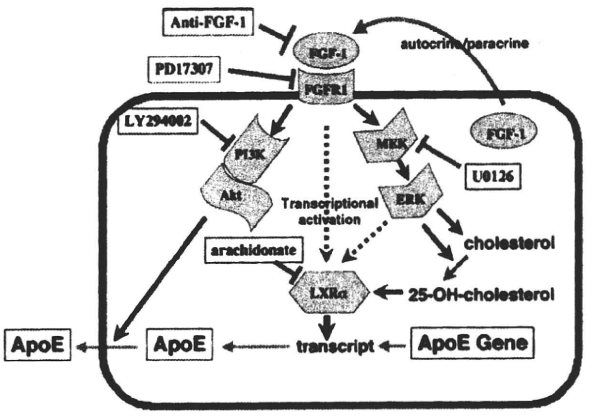

Fig. 8. A schematic model for mechanism by FGF-1 to increase production of apoE-HDL in rat astrocytes. The results from the references (14, 15) and those of this study are summarized.

Since LXRα was shown autoregulated in induction of apoE in mouse adipose tissue (42), the increase of LXRα by FGF-1 can also be through the same mechanism in rat astrocytes. However, FGF-1 also induces expression of the apoE gene apparently in a manner independent of stimulation of cholesterol biosynthesis (15), and this may be consistent with the current result that induction by FGF-1 of the LXRα gene partially remains after inhibition of the MEK/ERK pathway or cholesterol biosynthesis. Further investigation is required to elucidate detail of the mechanism for this cholesterol-independent pathway. It also remains unsolved how FGF-1 enhances apoE secretion by using the PI3K/Akt pathway (15). The results of this article together with our previous works (14, 15) are summarized in **Fig. 8.** Although human apoE gene is also upregulated through LXRs, it has not directly been demonstrated that FGF-1 plays a similar role in acute regulation of apoE-HDL production in the human brain. Studies should be conducted in human astrocytes in appropriate experimental systems.

REFERENCES

1. Curtiss, L. K., and W. A. Boisvert. 2000. Apolipoprotein E and atherosclerosis. *Curr. Opin. Lipidol.* **11:** 243–251.
2. Mazzone, T. 1996. Apolipoprotein E secretion by macrophages: its potential physiological functions. *Curr. Opin. Lipidol.* **7:** 303–307.
3. Pitas, R. E., J. K. Boyles, S. H. Lee, D. Foss, and R. W. Mahley. 1987. Astrocytes synthesize apolipoprotein E and metabolize apolipoprotein E-containing lipoproteins. *Biochim. Biophys. Acta.* **917:** 148–161.
4. Nakai, M., T. Kawamata, T. Taniguchi, K. Maeda, and C. Tanaka. 1996. Expression of apolipoprotein E mRNA in rat microglia. *Neurosci. Lett.* **211:** 41–44.
5. Ito, J., and S. Yokoyama. 2004. Roles of glia cells in cholesterol homeostasis in the brain. *In* Non-Neural Cells of the Nervous System: Function and Dysfunction, L. Hertz, editor. Elsevier: Amsterdam, The Netherlands. 519–534.
6. Boyles, J. K., R. E. Pitas, E. Wilson, R. W. Mahley, and J. M. Taylor. 1985. Apolipoprotein E associated with astrocytic glia of the central nervous system and with nonmyelinating glia of the peripheral nervous system. *J. Clin. Invest.* **76:** 1501–1513.
7. Muller, H. W., P. J. Gebicke-Harter, D. H. Hangen, and E. M. Shooter. 1985. A specific-37,000-dalton protein that accumulates in regenerating but not in nonregenerating mammalian nerves. *Science.* **228:** 499–501.
8. Dawson, P. A., N. Schechter, and D. L. Williams. 1986. Induction of rat E and chicken A-I apolipoproteins and mRNAs during optic nerve degeneration. *J. Biol. Chem.* **261:** 5681–5684.
9. Ignatius, M. J., P. J. Gebicke-Harter, J. H. P. Skene, J. W. Schilling, K. H. Weisgraber, R. W. Mahley, and E. M. Shooter. 1986. Expression of apolipoprotein E during nerve degeneration and regeneration. *Proc. Natl. Acad. Sci. USA.* **83:** 1125–1129.
10. Snipes, G. J., C. B. McGuire, J. J. Norden, and J. A. Freeman. 1986. Nerve injury stimulates the secretion of apolipoprotein E by non-neuronal cells. *Proc. Natl. Acad. Sci. USA.* **83:** 1130–1134.
11. Aoki, K., T. Uchihara, N. Sanjo, A. Nakamura, K. Ikeda, K. Tsuchiya, and Y. Wakayama. 2003. Increased expression of neuronal apolipoprotein E in human brain with cerebral infarction. *Stroke.* **34:** 875–880.
12. Tada, T., J. Ito, M. Asai, and S. Yokoyama. 2004. Fibroblast growth factor 1 is produced prior to apolipoprotein E in the astrocytes after cryo-injury of mouse brain. *Neurochem. Int.* **45:** 23–30.
13. Ueno, S., J. Ito, Y. Nagayasu, T. Furukawa, and S. Yokoyama. 2002. An acidic fibroblast growth factor-like factor secreted into the brain cell culture medium upregulates apoE synthesis, HDL secretion and cholesterol metabolism in rat astrocytes. *Biochim. Biophys. Acta.* **1589:** 261–272.
14. Ito, J., Y. Nagayasu, R. Lu, A. Kheirollah, M. Hayashi, and S. Yokoyama. 2005. Astrocytes produce and secrete FGF-1, which promotes the production of apoE-HDL in a manner of autocrine action. *J. Lipid Res.* **46:** 679–686.
15. Ito, J., Y. Nagayasu, K. Okumura-Noji, R. Lu, T. Nishida, Y. Miura, K. Asai, A. Kheirollah, S. Nakaya, and S. Yokoyama. 2007. Mechanism for FGF-1 to regulate biogenesis of apolipoprotein E-high density lipoprotein in astrocytes. *J. Lipid Res.* **48:** 2020–2027.
16. Ito, J., Y. L. Zhang, M. Asai, and S. Yokoyama. 1999. Differential generation of high-density lipoprotein by endogenous and exogenous apolipoproteins in cultured fetal rat astrocytes. *J. Neurochem.* **72:** 2362–2369.
17. Hossain, M. A., M. Tsujita, F. J. Gonzalez, and S. Yokoyama. 2008. Effects of fibrate drugs on expression of ABCA1 and HDL biogenesis in hepatocytes. *J. Cardiovasc. Pharmacol.* **51:** 258–266.
18. Fung, W. P., G. J. Howlett, and G. Schreiber. 1986. Structure and expression of the rat apolipoprotein E gene. *J. Biol. Chem.* **261:** 13777–13783.
19. Suzuki, S., T. Nishimaki-Mogami, N. Tamehiro, K. Inoue, R. Arakawa, S. Abe-Dohmae, A. R. Tanaka, K. Ueda, and S. Yokoyama. 2004. Verapamil increases the apolipoprotein-mediated release of cellular cholesterol by induction of ABCA1 expression via Liver X receptor-independent mechanism. *Arterioscler. Thromb. Vasc. Biol.* **24:** 519–525.
20. Iwamoto, N., S. Abe-Dohmae, R. Sato, and S. Yokoyama. 2006. ABCA7 expression is regulated by cellular cholesterol through the SREBP2 pathway and associated with phagocytosis. *J. Lipid Res.* **47:** 1915–1927.
21. Laffitte, B. A., J. J. Repa, S. B. Joseph, D. C. Wilpitz, H. R. Kast, D. J. Mangelsdorf, and P. Tontonoz. 2001. LXRs control lipid-inducible expression of the apolipoprotein E gene in macrophages and adipocytes. *Proc. Natl. Acad. Sci. USA.* **98:** 507–512.
22. Whitney, K. D., M. A. Watson, J. L. Collins, W. G. Benson, T. M. Stone, M. J. Numerick, T. K. Tippin, J. G. Wilson, D. A. Winegar, and S. A. Kliewer. 2002. Regulation of cholesterol homeostasis by the liver X receptors in the central nervous system. *Mol. Endocrinol.* **16:** 1378–1385.
23. Ou, J., H. Tu, B. Shan, A. Luk, R. A. DeBose-Boyd, Y. Bashmakov, J. L. Goldstein, and M. S. Brown. 2001. Unsaturated fatty acids inhibit transcription of the sterol regulatory element-binding protein-1c (SREBP-1c) gene by antagonizing ligand-dependent activation of the LXR. *Proc. Natl. Acad. Sci. USA.* **98:** 6027–6032.
24. Russell, D. W. 2000. Oxysterol biosynthetic enzymes. *Biochim. Biophys. Acta.* **1529:** 126–135.
25. Zechner, R., R. Moser, T. C. Newman, S. K. Fried, and J. L. Breslow. 1991. Apolipoprotein E gene expression in mouse 3T3–L1 adipocytes and human adipose tissue and its regulation by differentiation and lipid content. *J. Biol. Chem.* **266:** 10583–10588.
26. Shih, S. J., C. Allan, S. Grehan, E. Tse, C. Moran, and J. M. Taylor. 2000. Duplicated downstream enhancers control expression of the human apolipoprotein E gene in macrophages and adipose tissue. *J. Biol. Chem.* **275:** 31567–31572.
27. Wang, L., G. U. Schuster, K. Hultenby, Q. Zhang, S. Andersson, and J. A. Gustafsson. 2002. Liver X receptors in the central nervous system: from lipid homeostasis to neuronal degeneration. *Proc. Natl. Acad. Sci. USA.* **99:** 13878–13883.
28. Liang, Y., S. Lin, T. P. Beyer, Y. Zhang, X. Wu, K. R. Bales, R. B. DeMattos, P. C. May, S. D. Li, X. C. Jiang, et al. 2004. A liver X receptor and retinoid X receptor heterodimer mediates apolipoprotein E expression, secretion and cholesterol homeostasis in astrocytes. *J. Neurochem.* **88:** 623–634.
29. Abildayeva, K., P. J. Jansen, V. Hirsch-Reinshagen, V. W. Bloks, A. H. Bakker, F. C. Ramaekers, J. de Vente, A. K. Groen, C. L. Wellington, F. Kuipers, et al. 2006. 24(S)-hydroxycholesterol participates in a liver X receptor-controlled pathway in astrocytes that regulates apolipoprotein E-mediated cholesterol efflux. *J. Biol. Chem.* **281:** 12799–12808.
30. Koldamova, R. P., I. M. Lefterov, M. Staufenbiel, D. Wolfe, S. Huang, J. C. Glorioso, M. Walter, M. G. Roth, and J. S. Lazo. 2005. The liver X receptor ligand T0901317 decreases amyloid beta production in vitro and in a mouse model of Alzheimer's disease. *J. Biol. Chem.* **280:** 4079–4088.
31. Jiang, X. C., T. P. Beyer, Z. Li, J. Liu, W. Quan, R. J. Schmidt, Y. Zhang, W. R. Bensch, P. I. Eacho, and G. Cao. 2003. Enlargement of high density lipoprotein in mice via liver X receptor activation requires apolipoprotein E and is abolished by cholesteryl ester transfer protein expression. *J. Biol. Chem.* **278:** 49072–49078.
32. Ornitz, D. M., and N. Itoh. 2001. Fibroblast growth factors. *Genome Biol.* **2:** 3005.1–3005.12.

33. Burgess, W. H., and T. Maciag. 1989. The heparin-binding (fibroblast) growth factor family of proteins. *Annu. Rev. Biochem.* **58:** 575–606.
34. Burke, D., D. Wilkes, T. L. Blundell, and S. Malcolm. 1998. Fibroblast growth factor receptors: lessons from the genes. *Trends Biochem. Sci.* **23:** 59–62.
35. Szebenyi, G., and J. F. Fallon. 1999. Fibroblast growth factors as multifunctional signaling factors. *Int. Rev. Cytol.* **185:** 45–106.
36. Olsnes, S., O. Klingenberg, and A. Wiedlocha. 2003. Transport of exogenous growth factors and cytokines to the cytosol and to the nucleus. *Physiol. Rev.* **83:** 163–182.
37. Prudovsky, I., A. Mandinova, R. Soldi, C. Bagala, I. Graziani, M. Landriscina, F. Tarantini, M. Duarte, S. Bellum, H. Doherty, et al. 2003. The non-classical export routes: FGF1 and IL-1alpha point the way. *J. Cell Sci.* **116:** 4871–4881.
38. Imamura, T., K. Engleka, X. Zhan, Y. Tokita, R. Forough, D. Roeder, A. Jackson, J. A. Maier, T. Hla, and T. Maciag. 1990. Recovery of mitogenic activity of a growth factor mutant with a nuclear translocation sequence. *Science.* **249:** 1567–1570.
39. Mak, P. A., B. A. Laffitte, C. Desrumaux, S. B. Joseph, L. K. Curtiss, D. J. Mangelsdorf, P. Tontonoz, and P. A. Edwards. 2002. Regulated expression of the apolipoprotein E/C-I/C-IV/C-II gene cluster in murine and human macrophages. A critical role for nuclear liver X receptors alpha and beta. *J. Biol. Chem.* **277:** 31900–31908.
40. Lund, E. G., J. M. Guileyardo, and D. W. Russell. 1999. cDNA cloning of cholesterol 24-hydroxylase, a mediator of cholesterol homeostasis in the brain. *Proc. Natl. Acad. Sci. USA.* **96:** 7238–7243.
41. Ramirez, D. M., S. Andersson, and D. W. Russell. 2008. Neuronal expression and subcellular localization of cholesterol 24-hydroxylase in the mouse brain. *J. Comp. Neurol.* **507:** 1676–1693.
42. Ulven, S. M., K. T. Dalen, J-Å. Gustafsson, and H. I. Nebb. 2004. Tissue-specific autoregulation of the LXR{alpha} gene facilitates induction of apoE in mouse adipose tissue. *J. Lipid Res.* **45:** 2052–2062.

Pharmacological inhibition of ABCA1 degradation increases HDL biogenesis and exhibits antiatherogenesis[S]

Reijiro Arakawa,* Maki Tsujita,* Noriyuki Iwamoto,* Chisato Ito-Ohsumi,* Rui Lu,* Chen-Ai Wu,* Kenji Shimizu,† Tomoji Aotsuka,† Hashime Kanazawa,† Sumiko Abe-Dohmae,* and Shinji Yokoyama[1],*

Department of Biochemistry,* Nagoya City University Graduate School of Medical Sciences, Nagoya 467-8601, Japan, and Nishi-Tokyo Research Center,† Aska Pharmaceutical Co. Ltd., Hamura, Tokyo 205-8501, Japan

Abstract **Expression of ABCA1 is regulated by transcription of the gene and calpain-mediated proteolytic degradation, and inhibition ABCA1 degradation results in increased ABCA1 and HDL biogenesis in vitro. We examined whether this approach could be a potential antiatherogenic treatment. Although probucol inhibits both the activity and degradation of ABCA1, its oxidized products, spiroquinone and diphenoquinone, reduce degradation of ABCA1 without inhibiting its activity or altering transcription of the ABCA1 gene. Accordingly, both compounds enhanced apolipoprotein A-I/ABCA1-dependent generation of HDL in vitro, and increased hepatic ABCA1 and plasma HDL without increasing antioxidant activity in plasma when given to rabbits. Both compounds also decreased vascular lipid deposition in cholesterol-fed rabbits. We therefore conclude that stabilization of ABCA1 against calpain-mediated degradation is a novel and potentially important strategy to increase HDL formation and prevent atherosclerosis. Spiroquinone and diphenoquinone are potential seeds for development of such drugs.**—Arakawa, R., M. Tsujita, N. Iwamoto, C. Ito-Ohsumi, R. Lu, C-A. Wu, K. Shimizu, T. Aotsuka, H. Kanazawa, S. Abe-Dohmae, and S. Yokoyama. **Pharmacological inhibition of ABCA1 degradation increases HDL biogenesis and exhibits antiatherogenesis.** ***J. Lipid Res.*** **2009.** 50: **2299–2305.**

Supplementary key words ATP binding cassette transporter A1 • high density lipoprotein • atherosclerosis • calpain • probucol

HDL plays a central role in the catabolic pathway of cholesterol by transporting it from extrahepatic cells to the liver for conversion to bile acids, and accordingly, is thought to be antiatherogenic. Apolipoprotein-mediated generation of new HDL from cellular lipids is one of the major events in the initial step of this pathway, cellular cholesterol release (1, 2). This reaction was found to be defective in genetic HDL deficiency, Tangier disease (3, 4), and mutations were identified in the gene of ABCA1 as the cause of this disorder (5–7).

Expression of ABCA1 is regulated at the transcriptional level and posttranslationally by calpain-mediated proteolysys. ABCA1 is stabilized against this degradation by helical apolipoproteins (8–10), and destabilized by unsaturated fatty acid (11) or excess unesterified cholesterol (12). Inhibition of calpain increases HDL formation by cultured cells (8), suggesting inhibition of proteolytic degradation of ABCA1 is a potential drug target for increasing HDL. ABCA1 degradation takes place intracellularly and its inhibition results in increased ABCA1 recycling to the cell surface (13). Direct inhibition of internalization of ABCA1 also causes its accumulation in the cell surface (13). HDL formation increases in both cases, indicating that it takes place at the cell surface (13). Inhibition of ABCA1 degradation or internalization would therefore be a potential strategy to increase HDL biogenesis for prevention and/or regression of atherosclerosis.

The hypolipidemic drug, probucol, is known to reduce plasma HDL (14) by inhibiting ABCA1-mediated HDL biogenesis (15) and producing a Tangier disease-like state (16). Interestingly, probucol causes not only inactivation of ABCA1 but also inhibits its degradation (17). We found in preliminary experiments that the crude oxidized products of probucol enhanced HDL formation by cultured cells rather than inhibiting it. Based on these findings, we

This work was supported by Grants-in-Aid from the Ministry of Education, Culture, Science, Sports and Technology of Japan and from Japan Health Science Foundation, and by the Program for Promotion of Fundamental Studies in Health Sciences of the National Institute of Biomedical Innovation.

Manuscript received 13 March 2009 and in revised form 29 April 2009 and in re-revised form 19 May 2009.

Published, JLR Papers in Press, May 20, 2009
DOI 10.1194/jlr.M900122-JLR200

Abbreviations: acLDL, acetylated LDL; apoA-I, apolipoprotein A-I; CETP, cholesteryl ester transfer protein; DQ, diphenoquinone; GFP, green fluorescence protein; SQ, spiroquinone; SR-B1, scavenger receptor class B type 1.

[1] To whom correspondence should be addressed:
e-mail: syokoyam@med.nagoya-cu.ac.jp

[S] The online version of this article (available at http://www.jlr.org) contains supplementary data in the form of five figures.

hypothesized that some of the compounds in this mixture may function as inhibitors of ABCA1 degradation without inhibiting its activity. We therefore investigated the functions of spiroquinone (SQ) and diphenoquinone (DQ), the two potential oxidatized metabolites of probucol (supplementary Material I) (18), in their ability to alter ABCA1 activity and degradation as well as HDL formation in vitro and in vivo, and to alter the development of atherosclerosis in a rabbit model.

MATERIALS AND METHODS

Cell lines and culture conditions

THP-1 cells were maintained in 10% fetal bovine serum-RPMI1640 (Sigma) in a humidified atmosphere of 5% CO_2 and 95% air at 37°C. Human monocytic cell line cells THP-1 were differentiated to macrophages (THP-1 macrophages) by culturing the cells at a density of 1.0×10^6 cells/ml in the presence of 3.2×10^{-7} M phorbol 12-myristate 13-acetate (Wako) for 24 h (8, 10). Balb/3T3 fibroblasts and HEK293 cells were maintained in 10% fetal bovine serum-DMEM (Sigma). The cells were seeded in culture plates at a density of 3×10^5 cells/ml and cultured for 3 days before use.

Treatment of cells with probucol and its metabolites

Probucol was purchased from Shiono Finesse Co., Ltd., Osaka, Japan. Its oxidant products, SQ and DQ, were synthesized and isolated by the oxidation of probucol (18) and by reduction of 2,6-di-*tert*-butylphenol (19), respectively. SQ and DQ were chemically stable under the experimental conditions used (details are described in supplementary Material I). Probucol, SQ, or DQ were delivered to cells either after incorporation into acetylated low density lipoprotein (acLDL) as a vehicle (15, 17) or directly as a solution in 2-butanol. Drug-containing acLDL was prepared as described previously (15). Briefly, human LDL was incubated with sonicated lipid microemulsion composed of egg phosphatidylcholine (Avanti), triolein (Wako), and the selected compound in the presence of lipoprotein-free human plasma fraction, reisolated by a dextran sulfate-cellulose column and ultracentrifugation, and acetylated with acetic anhydride. The final preparation contained approximately 0.3 μg of the respective compound per 100 μg protein. THP-1 macrophages were preloaded with probucol or metabolites by incubating with the acLDLs for 24 h. The compounds were alternatively delivered to cells by adding them from stock solutions in 2-butanol to produce a final solvent concentration in the culture medium of 0.5%.

Cellular lipid release by ApoA-I

Apolipoprotein (apo)A-I was isolated from the human HDL fraction as described previously (20). THP-1 macrophages were preloaded with probucol, SQ, or DQ by incubating the compound-containing acLDL and incubated in media containing 0.2% BSA (Sigma) and 10 μg/ml of apoA-I for 24 h. The compounds were also given as a 2-butanol solution as mentioned above by incubating the cells in the presence of the compounds and apoA-I for 24 h. Cholesterol and choline-containing phospholipids released into the media were measured enzymatically (Wako) (21). The cells were dissolved in 0.1N NaOH for protein determination by bicinchoninic acid (BCA) method (Pierce).

Western blotting

After the cells were incubated to load the compounds, they were suspended in 5 mM Tris-HCl buffer (pH 8.5) containing protease inhibitor cocktail (Sigma) and placed on ice for 30 min. The cell suspension was centrifuged at 650 *g* for 5 min, and the supernatant was centrifuged at 105,000 *g* for 30 min to precipitate the total membrane fraction. Twenty μg wet-weight liver specimens of the rabbits were treated in the same manner as preparation of the membrane fraction. Protein in these fractions was analyzed by Western blotting using specific polyclonal antibodies against ABCA1 (8), scavenger receptor class B type 1 (SR-B1; Novus Biologicals), and β-actin (Sigma) and visualized by a chemiluminescence method (Amersham Life Science).

Real time quantitative PCR

ABCA1 mRNA was measured by using probes previously reported for human and mouse (8) in a 7300 Real Time PCR System (Applied Biosystems). Cultured cells were lysed in the presence of phenol and guanidine thiocyanate. cDNAs were synthesized by SuperScript™ First-Strand Synthesis Systems (Invitrogen). For rabbit ABCA1, total RNA was purified from rabbit liver and cDNA was synthesized as described above. A partial sequence of ABCA1 was amplified with synthetic oligonucleotide primers (5′-ACA ATA GTT GTA CGA ATA GCA GGG-3′, 5′-CTC ATC CTG TAG AAA AGA TGT GAG-3′) and cloned into pGEM®-T Easy Vector (Promega). Because the sequence of the partial clone of rabbit ABCA1 analyzed by a capillary sequencer 3100 (ABI) was 97% homologous to human ABCA1, these primers were used for the real-time quantitative PCR. ABCA1 expression was standardized to glyceraldehyde-3-phosphate dehydrogenase and β-actin.

Metabolic analysis of ABCA1

To examine degradation of ABCA1, THP-1 macrophages or Balb/3T3 cells were incubated for 24 h with 9-*cis*-RA (Sigma) to increase the expression of ABCA1 and treated with SQ or DQ for 30 min in 0.2% BSA-RPMI1640. Cells were washed once with PBS and incubated in 0.2% BSA-RPMI1640 containing 140 μM cycloheximide (Sigma) for the indicated periods, and ABCA1 protein analyzed by Western blotting as described above (8). ABCA1 in the cell surface was analyzed by biotinylation of the surface protein and its precipitation with avidin-beads followed by Western blotting (13). Internalization of ABCA1 was analyzed by biotinylation of surface ABCA1 and cleavage of the biotinylation of ABCA1 that remains in the surface after incubation as described elsewhere (13). To visualize intracellular localization of ABCA1, an expression vector containing ABCA1-green fluorescent protein (GFP) hybrid cDNA was transfected and expressed in HEK293 cells as described previously (22). Expression of ABCA1-GFP protein was confirmed by Western blotting with anti-ABCA1 antibody and with anti-GFP antibody. Intracellular localization of ABCA1-GFP was visually demonstrated as fluorescence images of the cells, placed on a 50-mm round coverslip for mounting in a temperature-controlled chamber at 37°C, and viewed with a LSM510 PASCAL laser scanning confocal microscope (Carl Zeiss). The averaged fluorescent intensity of ABCA1 in the plasma membrane was measured for 60 randomly selected cells using the software of the LSM510 PASCAL microscope.

Animal experiments

Three-month-old male New Zealand White rabbits were fed with LRC-4 diet containing SQ and DQ for 7 days. Plasma lipoproteins were analyzed for HDL and nonHDL fractions separated by ultracentrifugation at densities above and below 1.063 g/ml. The purity of each fraction was verified by agarose electrophoresis, and its cholesterol was measured by the enzymatic method. Expression of ABCA1 in the liver was determined by quantitative PCR for mRNA and by Western blotting for protein as described

above. For high-cholesterol experiments, 3-month-old male New Zealand White rabbits were fed with 0.5% cholesterol-containing diet supplemented with SQ or DQ for 8 weeks. Plasma lipoproteins were measured as described above and also analyzed by HPLC as previously described at Skylight Biotech, Tokyo, Japan (23). Aortas were extracted and fixed with 10% neutral buffered formalin solution and lipid deposition in the intima was stained with Oil Red O. The antiatherogenic effect of the drugs was evaluated by measuring the Oil Red O-stained area in the thoracic and abdominal regions. The digitized images were analyzed using Adobe Photoshop and NIH Image to estimate the relative area of lipid deposition.

Antioxidant activity in plasma

To measure antioxidant activity of the compounds in vivo, 3-month-old WHHL rabbits were fed LRC4 diet containing SQ or probucol for 1 month. Five μl of the serum was used for estimation of the antioxidant activity by evaluating its activity to reduce Cu^{2+} to Cu^{+} by measuring absorbance at 490 nm of a stable complex of Cu^{+}/bathocuproine (24) based upon the principle developed by MED.DIA, Italy, and modified by the Japan Institute for The Control of Aging, Nikken SEIL Corporation, according to the manufacture's instruction.

CETP mass in plasma

Cholesteryl ester transfer protein (CETP) mass in rabbit plasma was measured by enzyme-linked immuno-sorbent assay as described previously (25) using an assay system provided from Sekisui Medical Co., Ltd. (Tokyo, Japan).

Other methods

Intensity of each electrophoretic band was digitally scanned and semi-quantified by using an EPSON GT-X700 and Adobe Photoshop software. Statistical analysis of the data was performed by one-way ANOVA followed by Scheffé's test. Values represent mean ± SD for at least three independent measurements.

RESULTS

Probucol, SQ, and DQ were incorporated into acLDL and fed to THP-1 macrophages and cellular lipid release by apoA-I was measured. Whereas release of cholesterol and phospholipid was inhibited by probucol (15, 17), SQ and DQ enhanced the lipid release (**Fig. 1A**). ABCA1 protein was markedly increased by probucol in spite of inhibition of HDL formation, consistent with our previous finding (17) (Fig. 1B). SQ and DQ also markedly increased ABCA1. Other downstream oxidant products of probucol, bisphenol and butylphenol (18), did so but to a lesser extent (data not shown). When the THP-1 macrophages preloaded with acLDL were incubated with SQ and DQ added in a 2-butanol solution, ABCA1 apparently increased in the initial 30 min of the incubation (Fig. 1C). The increase in ABCA1 by SQ and DQ was also apparent in the presence of apoA-I (Fig. 1D), previously shown to inhibit calpain-mediated ABCA1 degradation (13). Similar effects in a dose-dependent manner were seen when SQ and DQ were given to THP-1 macrophages or Balb/3T3 mouse fibroblasts in a 2-butanol solution (supplementary Fig. IA, IB). However, the message of ABCA1 was not influenced by either compound (supplementary Fig. IC), similar to the previous finding with probucol (17). The amount of SQ and DQ in the cells was below the limit of our detection method (1 ng) (supplementary Material I) because of the low concentration of compounds and relatively small number of cells used in the experimental conditions.

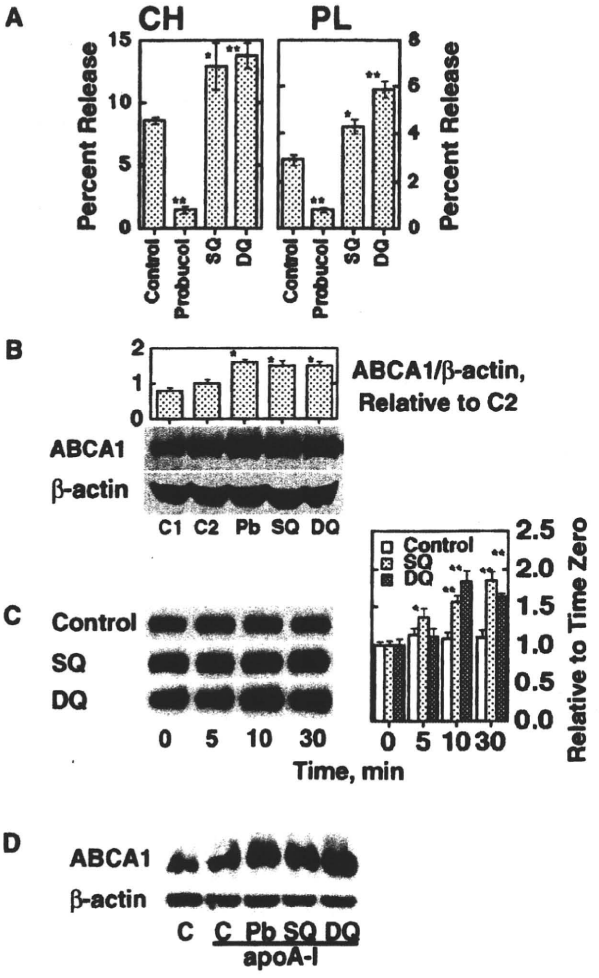

Fig. 1. The effect of probucol, spiroquinone (SQ) or diphenoquinone (DQ) in THP-1 macrophages. A: Cellular lipid release by apoA-I. Cells were incubated with acLDL containing each compound for 24 h at 100 μg/ml protein as 1.9 μM probucol, 2.0 μM SQ, and 2.4 μM DQ and incubated with 10 μg/ml apoA-I for another 24 h. Cholesterol (CH) and phospholipid (PL) in the medium were determined. B: ABCA1 protein in the same condition. Controls (C1 and C2) represent absence and presence of control acLDL. The numbers represent band intensity relative to C2. C: Time-dependent increase of ABCA1 after SQ and DQ were added as a 2-butanol solution (25 nM and 0.05 nM, respectively). The graph represents band intensity relative to time zero. D: Increase of ABCA1 by treatment with SQ and DQ (25 nM and 0.05 nM for 3 h) in the presence of 10 μg/ml apoA-I in the medium. The data represent the mean ± SE for three samples. * $P < 0.05$, ** $P < 0.01$ in comparison to control (A), C2 (B), and time zero (C).

Figure 2, A and B, shows the decay of ABCA1 in the presence of cycloheximide. Both SQ and DQ apparently retarded this process in a very similar manner to the effect observed with probucol (17). Figure 2C demonstrates inhibition of ABCA1 internalization by these compounds.

JOURNAL OF LIPID RESEARCH ASBMB

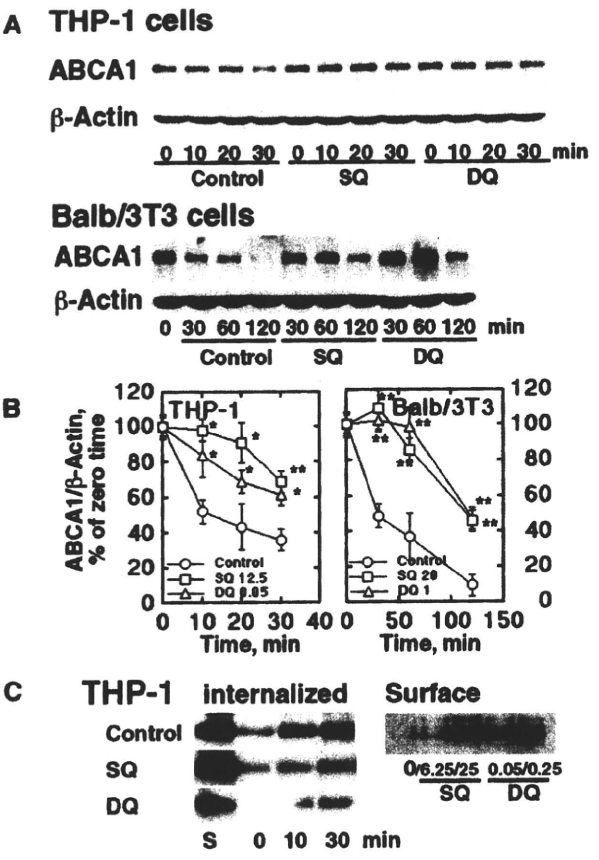

Fig. 2. Stabilization of ABCA1 by SQ and DQ. A: Retarded degradation of ABCA1 in the presence of cycloheximide in THP-1 macrophages and Balb/3T3 cells, by SQ (25 nM for THP-1 and 20 nM for Balb/3T3) and DQ (0.05 nM and 1.0 nM). B: Graphic expression of the results typically represented by Fig. 2A after standardization for β-actin. Error bars indicate SE for three measurements. Significant difference from control at each time point is indicated as * $P < 0.05$ and ** $P < 0.01$. C: Internalization of ABCA1. Left panel: THP-1 cells were preincubated with SQ (25 nM) and DQ (0.25 nM) for 16 h to equilibrate the cells with the compounds. The surface ABCA1 was then labeled by biotinylatin and the cells were incubated for time indicated. The surface biotinylation was cleaved and the remaining biotinylated ABCA1 was analyzed as the protein internalized. Right panel: Cell surface ABCA1 was analyzed by surface biotinylation after incubation with SQ and DQ (as indicated in nM) for 1 h.

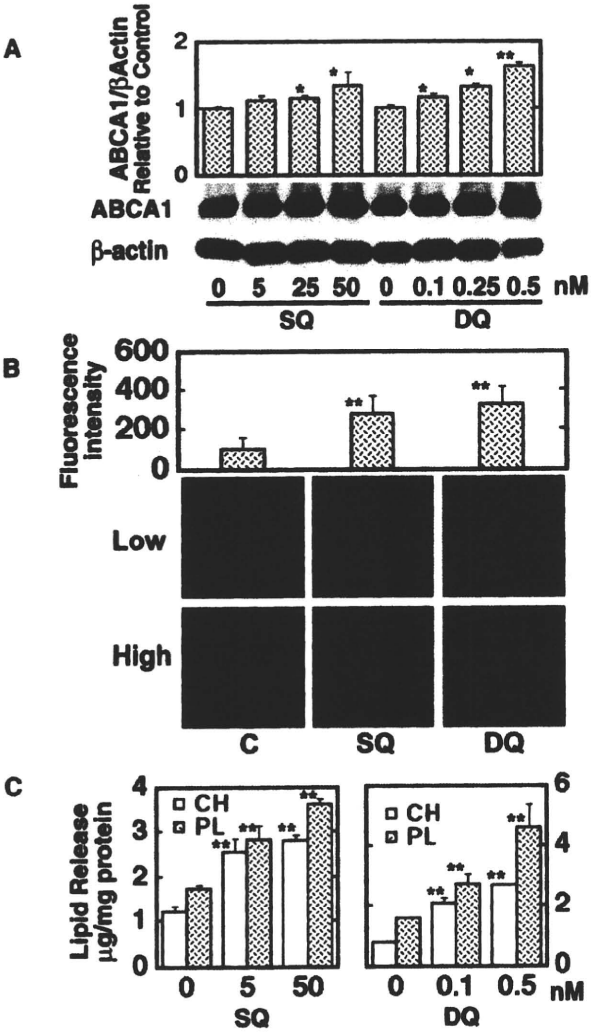

Fig. 3. Intracellular localization of ABCA1-GFP in HEK293 cells. A: HEK293 cells with stable expression of ABCA1-GFP were cultured with each compound (SQ 50 nM, DQ 0.5 nM) for 12 h. Cellular ABCA1-GFP was analyzed by using anti-ABCA1 antibody. B: Fluorescent image of the living cells was viewed with a laser scanning confocal microscope. The averaged fluorescent intensity in plasma membrane was measured by using the software of the LSM5 Pascal microscope. Sixty cells were analyzed in each group. (low magnitude and high magnitude). C: Release of cholesterol (CH) and phospholipid (PL) by 10 μg/ml apoA-I during the 12-h incubation. The data represent the mean ± SE for three measurements. * $P < 0.05$, ** $P < 0.01$ in comparison to each control.

Internalization of surface ABCA1 prelabeled by biotinylation was inhibited by SQ and DQ shown in the left panel. In contrast, ABCA1 in the cell surface was increased by these compounds, shown in the right panel. Inhibition of ABCA1 degradation by these compounds was thus shown to be by inhibiting internalization of ABCA1 (13). The effect of SQ and DQ on intracellular localization of ABCA1 was further examined by using HEK293 cells in which ABCA1-GFP was overexpressed. **Figure 3A** shows an increase of transfected ABCA1-GFP by SQ and DQ. Fig. 3B shows an increase of fluorescence intensity of ABCA1-GFP as well as images of its intracellular localization. SQ and DQ increased the fluorescence intensity at the cellular surface. In these conditions, SQ and DQ also increased the release of cellular lipid by apoA-I (Fig. 3C).

SQ and DQ were given to rabbits to examine their in vivo effects. **Figure 4A** shows an increase in plasma HDL-cholesterol and of hepatic ABCA1 protein (also in supplementary Fig. II) by SQ and DQ, with no increase in hepatic ABCA1 mRNA. Because probucol has strong antioxidant activity and its antiatherosclerotic effects are assumed to be due to this function, antioxidant activity of SQ, which supposedly has higher antioxidant activity than other

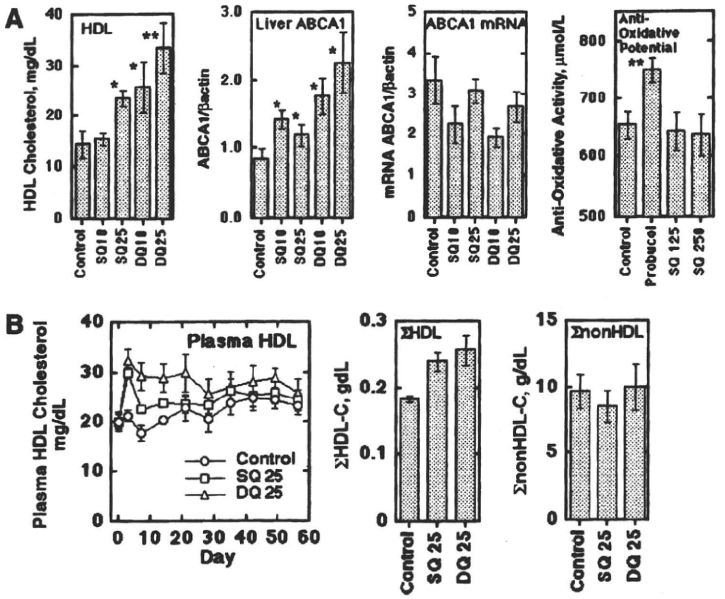

Fig. 4. Effects of SQ and DQ on rabbit plasma lipoproteins. A: The compounds were orally given (mg/kg/day, n = 4) and HDL-cholesterol was measured at day 3. Hepatic ABCA1 protein and mRNA were analyzed at day 7. Plasma antioxidant activity was determined for the animals given 330 mg/kg/day probucol and 125 and 250 mg/kg/day SQ for 1 month. DQ was given in a higher relative dose to SQ than in the in vitro studies because of less solubility in oil, indicating poor absorption. B: Long term effects of SQ and DQ on plasma HDL-cholesterol. SQ or DQ, 25 mg/kg/day, was given to the animals fed with 0.5% cholesterol diet for 8 weeks (n = 8 in each group). Left panel: Plasma HDL-cholesterol. Middle panel: Integrated HDL-cholesterol as sum of HDL-cholesterol for the test period (day 3 and at every week thereafter). Right panel: Integrated nonHDL-cholesterol estimated similarly to HDL. The data represent the mean ± SE. * $P < 0.05$, ** $P < 0.01$ in comparison to each control.

probucol oxidation products, has been examined in vivo in comparison to probucol. Although antioxidant activity in plasma was substantially increased in the probucol-treated animals, no significant change was found in plasma antioxidant activity with a higher dose of SQ (Fig. 4A). Figure 4B and supplementary Fig. III show the results in cholesterol-fed rabbits for 8 weeks. Treatment with SQ and DQ did not cause significant change in food intake and body weight (supplementary Fig. IIIA). SQ and DQ increased HDL-cholesterol shown in a time course and in its integrated values for the entire experimental term of 8 weeks (Fig. 4B), as well as in the profile of the HPLC analysis (supplementary Fig. IIIB). SQ and DQ induced a significant increase in HDL-cholesterol, whereas neither compound caused significant change in nonHDL lipoprotein-cholesterol. The HDL-increasing effect seemed somewhat diminished after the 4-week treatment. Plasma CETP markedly increased with cholesterol feeding but did not show a difference among the treatment groups (supplementary Fig. IV). The increase in ABCA1 protein in the liver by SQ or DQ was retained at the end of the experiment, whereas SR-B1 protein showed no change (supplementary Fig. IV). There was no apparent adverse effect in the animals.

Figure 5 shows the effects of SQ and DQ on the vascular lesions in the cholesterol-fed rabbits characterized as above. Lipid deposition in aortic intima was examined by Oil Red O staining. Relative lipid deposit area was 0.46 ± 0.19 for the controls versus 0.27 ± 0.09 and 0.29 ± 0.13 for the SQ and DQ treatment groups (P= 0.02 and 0.03 against the control), respectively, including the aortic arch regions (supplementary Fig. V). The evaluation for the arch regions, however, may be inaccurate and unreliable as the wall cannot be set flat for photographs, so that further quantitative analysis was performed for the thoracic and abdominal regions of aorta (Fig. 5A). The lesion area was significantly decreased by SQ (Fig. 5B, left). When the lesion area was standardized for the integrated value of non-HDL cholesterol in an individual animal, the reduction in lipid deposition was significant for both SQ and DQ

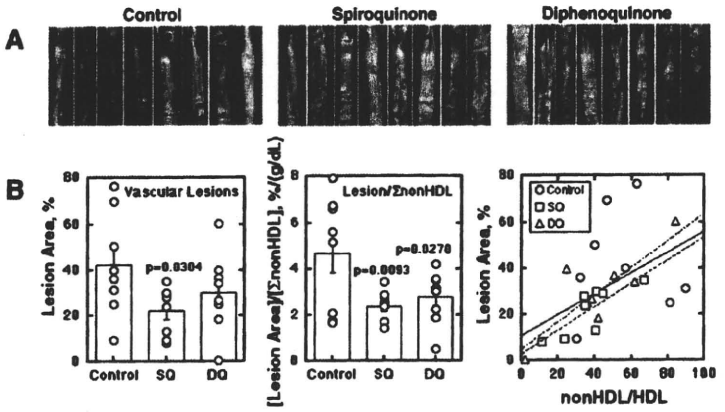

Fig. 5. Effects of SQ and DQ on vascular lipid deposit in cholesterol-fed rabbits. After 8 weeks of the experiments described in Fig. 4, lipid deposit in the aortic wall was evaluated by Oil Red O staining. A: Lipid deposit in the thoracic and abdominal aorta. B: Digitalized images were analyzed by an image processing software. Left panel: The lesion relative area (%). Middle panel: The relative lesion area standardized by the integrated nonHDL-cholesterol in each animal. Right panel: Plot of the relative lesion area (%) against the index of (integrated non-HDL-cholesterol)/(integrated HDL-cholesterol). Solid line represents fitting for all the groups ($y = 0.46 x + 11.2$, $r = 0.528$); even-broken line for the SQ-fed group ($y = 0.51 x + 3.3$, $r = 0.81$); and uneven-broken line for the DQ group ($y = 0.59 x + 5.2$, $r = 0.83$).

treatment (Fig. 5B, middle). Lipid deposition was a function of (nonHDL-cholesterol)/(HDL-cholesterol) to yield similar parameters in linear regression for each SQ and DQ treatment group and total (Fig. 5B, right), so that the effect of SQ and DQ on the lipid deposition may be attributed to the increase of HDL in association with stabilization of ABCA1.

DISCUSSION

To examine whether inhibition of ABCA1 degradation increases HDL formation and plasma HDL level, we attempted to screen potential candidate chemicals that inhibit degradation of ABCA1, including oxidized products of the ABCA1 inactivator probucol (18). In our preliminary experiments, crude oxidative products of probucol increased cellular HDL formation rather than decreased it. Treatment of cells with SQ and DQ were found to increase ABCA1 protein and apoA-I-mediated HDL formation. Both compounds stabilized ABCA1 against calpain-mediated degradation without changing its transcription. They also increased expression of ABCA1-GFP in HEK293 cells expressing ABCA1-GFP with a nonphysiological promoter. The compounds increased plasma HDL in rabbits by increasing hepatic ABCA1 and suppressed lipid deposition in the arterial wall of cholesterol-fed rabbits. Thus, we conclude that these compounds increase HDL formation through protecting ABCA1 from degradation and thereby reduce atherogenesis in the experimental animals. The effects were apparently independent of antioxidant activity, previously considered to be one of the major antiatherogenic properties of probucol in similar animal models (26, 27), because these compounds did not exhibit significant antioxidant activity in plasma.

We thus demonstrated that pharmacologic inhibition of ABCA1 degradation could increase ABCA1 and plasma HDL and counteract atherogenesis in a model of hypercholesterolemia in vivo. SQ and DQ were shown to cause retardation of ABCA1 degradation seemingly by inhibiting internalization of ABCA1, a prerequisite for calpain-mediated proteolysis (13), rather than by direct inhibition of the calpain reaction. At this stage, we do not have further mechanistic insight into the action of SQ and DQ. The effects might be similar to the effect of cytochalasin D observed in vitro in cultured cells, including an increase of ABCA1 in the cell surface even under conditions where ABCA1 degradation was retarded by the presence of apoA-I (13). Because both SQ and DQ are extremely hydrophobic and likely incorporated into the membrane, these compounds may induce conformational alteration of ABCA1 to stabilize it against internalization for its degradation. However, it is unclear whether SQ and DQ by themselves cause such an effect or their metabolites may secondarily do so. Indeed, such products as bisphenol and butylphenol did show similar activity, but to a lesser extent, as described in the results section. This point should further be examined. It is interesting that probucol inactivates ABCA1 for HDL formation while inhibiting ABCA1 degradation but SQ and DQ only induce the latter effect. There may be a hint in this discrepancy to solve the question on the reaction mechanism of these compounds.

The results demonstrated here showed a novel concept for drug development, enhancement of the function of a specific membrane protein such as transporters or receptors by inhibiting their biological degradation. SQ, DQ, or their related compounds can thus be potential drug candidates to increase HDL formation and prevention/cure of atherosclerosis by inhibiting ABCA1 degradation. Several issues remain to be addressed. The compounds are extremely hydrophobic and need to be improved for oral administration. The apparent tendency to diminish the HDL-raising effect over time may be a problem for long-term administration. Probucol has been used in the market for years, and SQ and DQ may be produced as its metabolites in vivo (18). Further investigation is still required for any unexpected in vivo effects of the compounds, such as their influence on metabolism of membrane proteins in general and the exact mechanism for inhibiting degradation of ABCA1. A wide and thorough survey is needed of their influence on gene expression.

Probucol decreases HDL by inhibiting the activity of ABCA1 (15–17, 28, 29). Despite this HDL-lowering effect, probucol was proposed to have specific antiatherosclerotic properties based on clinical findings of efficient regression of cutaneous and tendinous xanthomas in familial hypercholesterolemia (30). It is also proposed to inhibit atherogenesis in experimental animals because of its ability to inhibit oxidation of LDL (26, 27, 31). We previously discovered that probucol inactivates ABCA1's ability to form HDL while inhibiting calpain-dependent degradation (17), the net result being a severe reduction in HDL. In contrast, we demonstrate here that oxidized products of probucol retain the ability to inhibit ABCA1 degradation but do not inhibit HDL formation by ABACA1. If SQ and/or DQ are produced during the in vivo oxidant metabolism of probucol, these products may induce an increase in active ABCA1 in some tissues. In addition to the effect on ABCA1, probucol has been proposed to induce an increase in activity of CETP (32) or SR-B1 (33) as the causes of the decrease of HDL. However, we found no change in SR-B1 protein by SQ or DQ in rabbit liver (supplementary Fig. IV) or in the mRNAs of apoA-I, LCAT, PLTP, or SR-B1 in the liver of the probucol-fed mice (16). Because the HDL-increasing effects of SQ and DQ were observed in mice as well in our preliminary experiments, the effect of SQ and DQ should not be related to CETP. CETP markedly increased in the rabbit plasma regardless of the drug administration by cholesterol feeding (34) (supplementary Fig. IV) and this effect might somewhat mask the specific increase of plasma HDL by SQ and DQ in this particular model.

The authors thank Tetsuya Murata, a medical student at Nagoya City University, for his contribution to the initial stage of this project. The authors are also grateful to Takako Sekine, Hisae Takayama, Tomoya Fujisawa, and Takeo Matsukura at Aska